

Copyright
by
Faisal Alammari
2020

The Thesis Committee for Faisal Alammari
Certifies that this is the approved version of the following Thesis:

**Wettability Altering Surfactants for High-Temperature Tight
Carbonate Reservoirs**

APPROVED BY
SUPERVISING COMMITTEE:

Kishore Mohanty, Supervisor

Wen Song

**Wettability Altering Surfactants for High-Temperature Tight
Carbonate Reservoirs**

by

Faisal Alammari

Thesis

Presented to the Faculty of the Graduate School of

The University of Texas at Austin

in Partial Fulfillment

of the Requirements

for the Degree of

Master of Science in Engineering

The University of Texas at Austin

August 2020

Dedication

To my loving parents, Latifah and Ghazi,
My sisters, Aisha and Sara.

Acknowledgements

I would like to express my gratitude to Dr. Kishore Mohanty for giving me the opportunity to work under his supervision and providing me with the perfect platform to conduct my research. Thank you for challenging me intellectually and finding the time to guide me through my research challenges. I would also like to extend my appreciation to Dr. Wen Song for her guidance and valuable feedback.

The unconditional support and invaluable mentorship I received from Dr. Chammi Miller greatly helped me achieve my research objectives. Thank you for always finding the time share your experiences and encourage me to think outside the box. I would also like to thank my fellow graduate students Haofeng Song, Yue Shi, and Jaebum Park, and the lab technician Saroj Ghimire for their endless support.

My appreciation extends to the Hildebrand Department of Petroleum & Geosystems Engineering at the University of Texas at Austin for providing me with the perfect environment to grow both academically and personally. I would like to acknowledge the management and academic advisors of my sponsors, Saudi Aramco, for granting me the opportunity to pursue higher education and tremendously supporting me throughout my studies. I also want to thank the sponsors of the chemical EOR project for their generosity.

Lastly, my caring family Latifah, Ghazi, Aisha, and Sara, thank you for your endless encouragement and support throughout this journey.

Abstract

Wettability Altering Surfactants for High-Temperature Tight Carbonate Reservoirs

Faisal Alammari, M.S.E

The University of Texas at Austin, 2020

Supervisor: Kishore Mohanty

The global growth in energy demand coupled with the natural decline in new discoveries place a great importance on maximizing oil recovery from the existing resources. Research on chemical enhanced oil recovery (CEOR), made viable through favorable economic conditions, can unlock significant amount of oil, and extend the life of mature reservoirs by several years. The application of CEOR on carbonate reservoirs, which host more than half the world's oil reserves, is especially attractive due to the usually low recovery factors from the primary and secondary recovery stages, ensuing from a multitude of unfavorable characteristics, one of which is the carbonates' tendency to be preferentially oil-wet.

The evaluated reservoir in this research is a tight limestone reservoir at 116 °C with a relatively high formation water hardness of 1,773 ppm. This combination of challenging properties is a limitation to many CEOR methods, especially those involving the use of polymer for mobility control, making wettability alteration an attractive approach under such conditions. This research provides a systematic framework to select,

screen, and test commercially available surfactants with various classes and distinct functional groups for their efficacy at altering the reservoir's wettability, thereby enhancing oil recovery.

Twenty different surfactants were rigorously evaluated on polished, oil-wet, outcrop discs that possess a similarity to the reservoir's mineralogic and petrophysical properties. The surfactants were then screened based on their efficiency at altering the wettability of the discs via the contact angle method. Seven surfactants successfully altered the carbonate's wettability from oil-wet to intermediate-wet or water-wet with a reduction in contact angle that ranged from 35° up to 94° . Spontaneous imbibition experiments were then carried out on oil-wet 3-in.-long core plugs immersed in these seven surfactants, where ultimate oil recovery was increased by up to five times. A repeat of the spontaneous imbibition experiments on reservoir core plugs indicated that the screening results are representative and scalable, whereby the recoveries were comparative between the two rock types.

Finally, a core flood experiment was conducted on a 1-ft.-long core using cetyltrimethylammonium chloride (CTAC), which was the best-performing surfactant in the screening experiments—reducing the contact angle from $145^{\circ} (\pm 5^{\circ})$ to $51^{\circ} (\pm 7^{\circ})$. The injection of 1.0 wt% CTAC solution in the tertiary recovery stage resulted in an incremental oil recovery (ΔS_o) of 19.6%. The results look promising, but additional experiments need to be conducted to establish the kinetics and the limitations of the process.

Table of Contents

List of Tables	xiii
List of Figures	xiv
CHAPTER 1 INTRODUCTION	17
1.1 Objective	17
1.2 Description of Chapters	17
CHAPTER 2 BACKGROUND AND LITERATURE REVIEW	19
2.1 Background	19
2.2 Chemical Enhanced Oil Recovery	20
2.3 Wettability	21
2.3.1 Wettability Quantification	21
2.3.2 Carbonates Wettability	22
2.3.3 Factors Affecting Carbonates Oil-Wetness	22
2.3.3.1 Acid Content	23
2.3.3.2 Crude Oil Composition	23
2.3.3.3 Ionic Composition of Brine	23
2.3.3.4 Temperature	24
2.3.3.5 Reservoir Mineralogy	25
2.3.4 Oil Retention Mechanism	25
2.3.4.1 Capillary Entrapment	26
2.3.4.2 Surface Trapping	27
2.3.5 The Effect of Wettability on Relative Permeability and Waterflood Efficiency	27

2.4 Surfactants	30
2.4.1 Surfactant Chemistry	30
2.4.1.1 Interfacial Tension	31
2.4.1.2 Critical Micelle Concentration (CMC)	32
2.4.1.3 The Effect of Surfactant Structure	33
2.4.2 Surfactant Application in EOR I: Wettability Alteration	36
2.4.2.1 Wettability Alteration Mechanisms	37
2.4.2.2 Spontaneous Imbibition	38
2.4.3 Surfactant Application in EOR II: Ultra Low IFT Micellar Flooding	39
CHAPTER 3 MATERIALS AND PROCEDURES	41
3.1 Materials	41
3.1.1 Crude Oil	41
3.1.2 Surfactants	41
3.1.3 Salts and Additives	43
3.1.4 Carbonate Rocks	43
3.2 Procedures	43
3.2.1 Brine Preparation	43
3.2.1.1 Total Dissolved Solids Measurement	43
3.2.1.2 pH Measurement	44
3.2.2 Crude Oil Preparation	44
3.2.2.1 Viscosity Measurement	44
3.2.3 Surfactant Solutions Preparation	44
3.2.4 Carbonate Discs Preparation	45

3.2.4.1 Carbonate Discs Aging	45
3.2.5 Initial Screening	45
3.2.5.1 Aqueous Stability Testing	45
3.2.5.2 CMC Determination.....	46
3.2.5.3 Wettability Screening.....	46
3.2.6 Contact Angle Measurement.....	47
3.2.7 Interfacial Tension Measurement	47
3.2.8 Spontaneous Imbibition	48
3.2.8.1 Spontaneous Imbibition Apparatus.....	48
3.2.8.2 Outcrop Core Plugs Preparation	49
3.2.8.3 Core Plug Cleaving	49
3.2.8.4 Reservoir Core Plugs Preparation	50
3.2.9 Core Floods	50
3.2.9.1 Core Holder.....	50
3.2.9.2 Accumulators	51
3.2.9.3 Pumps.....	51
3.2.9.4 Pressure Transducers	51
3.2.9.5 Fraction Collectors.....	52
3.2.9.6 Core Preparation	52
3.2.9.7 Core Flood Setup	52
3.2.9.8 Oil Flooding	53
3.2.9.9 Core Aging.....	54
3.2.9.10 Waterflooding	54

3.2.9.11 Surfactant Flooding.....	54
3.2.9.12 Effluent Analysis	55
3.3 Calculations	55
3.3.1 Spontaneous Imbibition Calculations	55
3.3.1.1 Plugs Pore Volume	55
3.3.1.2 Oil Recovery Factor	55
3.3.1.3 Time-Scaling.....	56
3.3.2 Core Flood Calculations	56
3.3.2.1 Physical Properties.....	56
3.3.2.2 Effective Porosity.....	56
3.3.2.3 Effective Permeability	57
3.3.2.4 Phase Saturation.....	57
3.3.2.5 End-Point Relative Permeability.....	57
3.3.2.6 Effluent Composition.....	58
3.3.2.7 Oil Recovery Factor.....	58
CHAPTER 4 RESULTS	59
4.1 Reservoir Characterization	59
4.1.1 Rock Properties.....	59
4.1.2 Brine Composition	61
4.1.3 Crude Oil Properties	62
4.2 Surfactant Screening	63
4.2.1 Aqueous Stability.....	63
4.2.2 Surface Tension	64

4.2.3 Wettability-Alteration Screening	66
4.2.4 Contact Angle Measurements	68
4.2.5 Interfacial Tension	70
4.3 Spontaneous Imbibition Experiments	71
4.3.1 Outcrop Core Plugs.....	71
4.3.1.1 Oil Recovery Rate.....	72
4.3.1.2 Plug Cleaving.....	78
4.3.2 Reservoir Core Plugs	83
4.3.2.1 Oil Recovery Rate.....	84
4.4 Core Floods.....	87
4.4.1 Core Description	87
4.4.2 Core Flood 1	88
CHAPTER 5 CONCLUSIONS	91
5.1 Systematic Screening & Testing.....	91
5.2 Wettability Alteration	92
5.3 Enhanced Oil Recovery	93
5.4 Future Work Recommendations	94
APPENDIX A – SCREENING PICTURES.....	96
REFERENCES	101

List of Tables

Table 3.1 – Surfactants used for wettability alteration	42
Table 4.1 – The mineralogy (wt%) of the outcrop and reservoir rocks	60
Table 4.2 – The ionic composition of the injection and formation brines	62
Table 4.3 – Crude oil composition (SARA Analysis)	63
Table 4.4 – Surfactants that failed the aqueous stability test.....	64
Table 4.5 – The CMC of aqueous stable surfactants	64
Table 4.6 – Results of the visual wettability alteration screening	67
Table 4.7 – The mean and standard deviation of the contact angle measurements for the control sample and the candidate surfactants.....	68
Table 4.8 – The oil/water interfacial tension of the control sample and the candidate surfactants at 100 °C	70
Table 4.9 – The physical and petrophysical properties of the spontaneous imbibition outcrop core plugs.....	71
Table 4.10 – The physical and petrophysical properties of the spontaneous imbibition reservoir core plugs.....	84
Table 4.11 – The physical and petrophysical properties of the core flooding core	88

List of Figures

Figure 2.1 – Idealized schematic of oil droplets on water-wet (left), intermediate-wet (middle), and oil-wet (right) surfaces.	22
Figure 2.2 – Idealized schematic of the relative permeability behavior in oil-wet (dashed) and water-wet (solid) systems.	28
Figure 2.3 – Idealized schematic of the waterflood efficiency in oil-wet (dashed) and water-wet (solid) systems.	29
Figure 2.4 – The chemical structure of cetyltrimethylammonium chloride (CTAC).	30
Figure 2.5 – The chemical structure of alkyl benzene sulfonate (ABS).	30
Figure 2.6 – The chemical structure of isotridecyl alcohol ethoxylate.	30
Figure 2.7 – The chemical structure of coco betaine (CB).	31
Figure 2.8 – Comparison of a surfactant solution below (left) and above (right) the CMC.....	32
Figure 2.9 – Idealized schematic of a surfactant’s CMC determination.....	33
Figure 3.1 – A sample of the outcrop carbonate discs used for wettability screening.	45
Figure 3.2 – The spontaneous imbibition apparatus.	49
Figure 3.3 – Core flooding setup	53
Figure 4.1 – Pore size distribution of the outcrop and reservoir rocks from MICP test.	61
Figure 4.2 – Example of a stable surfactant (left, 0.5 wt% BTC [®] 8358) and unstable surfactant (right, 0.5 wt% Calimulse [®] PR).	63
Figure 4.3 – Surface tension as a function of surfactant concentration at room temperature for three sample surfactants.	65
Figure 4.4 – Oil-wet carbonate disc immersed in injection brine.....	66

Figure 4.5 – Two carbonate discs immersed in Ethoquad® 0/12 PG (left) and ASPIRO® S-2430x (Right).	68
Figure 4.6 – Representative contact angle of the control sample and the surfactants that showed significant wettability alteration.	69
Figure 4.7 – The reproducibility of the contact angle measurements.	69
Figure 4.8 – The oil recovery rate from the oil-wet outcrop core plugs.	72
Figure 4.9 – The relationship between the contact angles and the oil recovery factors at the end of the spontaneous imbibition experiments.	73
Figure 4.10 – Comparison of the core plug immersed in Benzalkonium Chloride on days 1, 2, and 45.	74
Figure 4.11 – Comparison between the core plugs immersed in CTAC, BTC® 8358, and Benzalkonium Chloride on day 2.	75
Figure 4.12 – Comparison of the plug immersed in BTC® 8358 at days 1, 2, and 45.	76
Figure 4.13 – Comparison of the top surface of the core plug immersed in BTC® 8358 at days 2 and 45.	76
Figure 4.14 – Comparison of the aqueous phase of four samples on the last day of spontaneous imbibition.	77
Figure 4.15 – Comparison of the core plug immersed in Mackam® CB-35 at days 1, and 45.	78
Figure 4.16 – The cleaved core plug immersed in ASPIRO® S-2430x.	79
Figure 4.17 – The cleaved core plug immersed in Phenol 2PO-60EO.	80
Figure 4.18 – The relationship between the oil recovery factor and the IFT of the nonionic surfactants.	80
Figure 4.19 – The relationship between the oil recovery factor and the contact angle of the nonionic surfactants.	81

Figure 4.20 – The cleaved core plug immersed in BTC [®] 8358.....	82
Figure 4.21 – The cleaved core plug immersed in Mackam [®] CB-35.....	83
Figure 4.22 – The oil recovery rate from the oil-wet reservoir core plugs.....	84
Figure 4.23 – Comparison between the recovery rates from the outcrop core plugs (solid) and the reservoir core plugs (dashed).....	85
Figure 4.24 – Comparison between the recovery rate from the outcrop plugs (solid) and the reservoir plugs (dashed) using non-dimensional time (t_D).....	86
Figure 4.25 – Core flood 1 effluent analysis.....	89
Figure 4.26 – Core flood 1 pressure drop.	90
Figure A1 – ASPIRO [®] S-2430x initial screening.....	96
Figure A2 – Calfax [®] 16-35 initial screening.	96
Figure A3 – ASPIRO [®] S-2410 initial screening.....	96
Figure A4 – CTAC initial screening.....	97
Figure A5 – BTC [®] 8358 initial screening.....	97
Figure A6 – Dowfax [®] 3B-2 initial screening.....	97
Figure A7 – Calfax [®] DB-45 initial screening.	98
Figure A8 – Mackam [®] CB-35 initial screening.....	98
Figure A9 – Ethoquad [®] 0/12 PG initial screening.....	98
Figure A10 – Stepanquat [®] 3712-W initial screening.....	99
Figure A11 – Benzalkonium Chloride initial screening.	99
Figure A12 – Phenol 2PO-60EO initial screening.....	99
Figure A13 – Phenol 2PO-70EO initial screening.....	100

CHAPTER 1 INTRODUCTION

1.1 OBJECTIVE

Carbonate reservoirs constitute half the world's known hydrocarbon reserves, yet the ultimate oil recovery from conventional water flooding processes leaves behind significant oil volumes. The unfavorable oil-wetness of most carbonate reservoirs is one of the detrimental factors (along with heterogeneity) that lead to oil retention by capillary entrapment and surface trapping in addition to reducing the oil relative permeability.

The high remaining oil saturation after water flooding makes carbonate reservoirs attractive prospects for chemical enhanced oil recovery (CEOR). Surfactants are used to enhance oil recovery from carbonates by altering their wettability from oil-wet to intermediate-wet or water-wet, thereby increasing the oil relative permeability and switching the sign of the capillary pressure required for water imbibition into oil-bearing pores. Surfactant-polymer formulations are also used to develop ultralow tension and thus mobilize oil; that process is not studied in this work.

This research systematically identifies and evaluates suitable single-surfactant systems to enhance oil recovery by altering a carbonate reservoir's wettability to a more favorable, preferentially water-wet state. The reservoir evaluated in this research is a tight, high-temperature limestone reservoir with a relatively high injection water hardness.

1.2 DESCRIPTION OF CHAPTERS

This thesis contains five chapters. Chapter 2 provides a literature review covering the fundamentals of wettability and surfactant chemistry. Chapter 3 outlines the experimental procedures and processes utilized throughout the research from initial

screening to core flood experiments. Chapter 4 discusses the results of the contact angle, imbibition, and coreflood experiments. Chapter 5 summarizes the conclusions and offers a way forward.

CHAPTER 2 BACKGROUND AND LITERATURE REVIEW

This chapter provides background information on the challenges posed by carbonate reservoirs, the factors affecting carbonates' wettability, and its impact on the recovery factor and waterflood efficiency. Finally, it supplies a literature review on the fundamentals of surfactant chemistry and its application in EOR processes.

2.1 BACKGROUND

Crude oil is responsible for supplying approximately one third of the world's current total energy demand. More importantly, the world's energy consumption, spurred by economic and population growth, is projected to grow by 50% by the year 2050 (2019 International Energy Outlook, the U.S. Energy Information Administration). The increase in demand places a greater importance on the role played by oil operators in continuing to ensure the world's energy security. As the annual rate of new discoveries naturally diminishes, maximizing recovery from the existing assets will become vitally important.

Carbonate reservoirs constitute around half the world's existing reserves (Roehl and Choquette, 1985; Akbar et al., 2000). Yet, the estimated ultimate oil recovery (EUR) from secondary recoveries with conventional water flooding is approximately 30-40% of the original oil in place (Wardlaw, 1996). The low recovery factor in carbonates is a result of the combined effect of poor microscopic and macroscopic displacement efficiencies (Marinque et al., 2006). Reservoirs heterogeneity, pore network complexity, wide and multimodal pore size distribution, presence of natural fractures, and unfavorable wettability are all factors contributing to this poor recovery. A combination of these factors can lead to oil retention by capillary entrapment, bypassing, channeling,

surface trapping, and fingering, thus leaving behind significant volumes of unrecovered oil.

The high remaining oil saturation left behind after water flooding makes carbonate reservoirs attractive candidates for enhanced oil recovery (EOR) processes, since the economic feasibility of an EOR project is mainly a function of incremental oil recovery relative to the chemical cost and any associated capital investment.

2.2 CHEMICAL ENHANCED OIL RECOVERY

The objective of tertiary oil recovery is to reduce the residual oil saturation and to produce part of the oil volumes that cannot be otherwise recovered by primary (e.g., gas cap expansion or bottom water aquifer) or secondary (e.g., waterflooding) recovery mechanisms. A tertiary recovery process that relies on the use of one or more chemicals is known as chemical enhanced oil recovery (CEOR). The use of chemicals facilitates the onset of oil mobilization, which hinges on altering the rock-fluid interactions, fluid-fluid interactions, applied pressure gradients, or relative phase volumes (Stegemeier, 1977).

The subject reservoir in this research is a tight limestone reservoir at 116 °C with a relatively high injection water hardness of 1,773 ppm. The high reservoir temperature, coupled with the high injection water hardness, limits the use of many chemicals due to their intolerance to such harsh conditions. More importantly, the low carbonate permeability (5-20 mD) presents a unique complexity that limits the use of polymers for mobility control since polymer transport through the small pore throat radii (under 1 μm) is not feasible without compromising its rheology (Ghosh et al., 2017). Furthermore, low-tension micellar flooding requires the injection of a polymer drive to preserve the microemulsion bank integrity (Healy and Reed, 1974; Nelson and Pope, 1978; Gupta and

Trushenski, 1979). Thus, for high temperature, high hardness, low permeability, carbonate reservoirs, wettability alteration is an attractive strategy for CEOR.

2.3 WETTABILITY

Wettability is the affinity of a rock's surface to one fluid in the presence of another immiscible fluid (Craig, 1971). In a crude oil-brine-rock (COBR) system, a water-wet rock has a higher affinity to water. Similarly, an oil-wet rock has a higher affinity to oil. The qualitative description of a rock's wettability can fall in a wide spectrum of different degrees of wetness that range from strongly water-wet to strongly oil-wet. A rock that retains a nearly equal affinity to either fluids is described as intermediate-wet. Many rocks are mixed-wet, where a part of the rock's surface is water-wet and another part is oil-wet (Salathiel, 1973).

2.3.1 Wettability Quantification

The rock's wettability can be quantitatively characterized by the Amott-Harvey index, USBM index, or contact angle method (Anderson, 1986b). The latter is used throughout this research. In a COBR system, the contact angle is the angle water creates on the rock surface in the presence of oil; it arises from the imbalance of forces resulting from the solid-water, solid-oil, and oil-water interfacial energies, i.e.,

$$\sigma_{ow} \cos \theta = \sigma_{os} - \sigma_{ws}$$

The contact angle is less than 75° on the rock surface in a water-wet system and greater than 105° in an oil-wet system. Angles between 75°-105° are indicative of an intermediate-wet system (Figure 2.1).

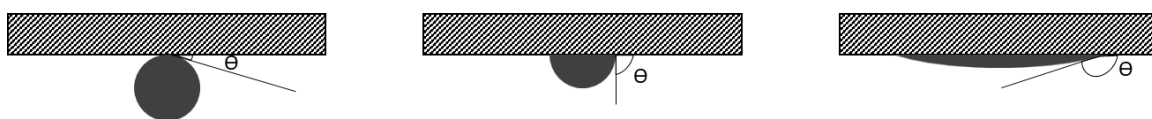


Figure 2.1 – Idealized schematic of oil droplets on water-wet (left), intermediate-wet (middle), and oil-wet (right) surfaces.

2.3.2 Carbonates Wettability

Most carbonate reservoirs are oil-wet or mixed-wet. In two independent studies, Treiber et al. (1972) and Chilingar and Yen (1983) found that at least 80% of the evaluated carbonate reservoirs are oil-wet. The wettability of a rock is a function of the stability of the connate water film coating the rock's surface, which is governed by the electric double layer (EDL) at the rock/water and oi/water interfaces (Hall et al., 1983; Blake and Kitchener, 1977). At slightly-above-neutral pH values typical of carbonate reservoirs, the rock/water interface retains a positive electrokinetic (zeta) potential due to the presence of the potential determining ion Ca^{2+} from calcite minerals (Buckley et al., 1989). On the other hand, the oil/water interface often retains a negative charge due to the dissociation of naphthenic and carboxylic acid groups in the crude oil. The opposite potentials result in a negative disjoining pressure that causes the two boundaries to attract. Consequently, the connate water film coating the rock's surface becomes unstable and eventually collapses. As a result, polar molecules in the crude oil can contact and strongly adsorb onto the carbonate surface leading to oil-wetness (Marrow, 1990).

2.3.3 Factors Affecting Carbonates Oil-Wetness

All reservoirs are initially water-wet, but there are numerous factors, both physical and chemical, that impact the onset and extent of oil-wetness in carbonate reservoirs (Anderson, 1986a). Some conditions are applicable over geologic timescales. Yet, most can be simulated in a laboratory setting.

2.3.3.1 Acid Content

The crude oil's acid content is defined by the acid number, described by the ATSM 664-89 as the amount of base required, in mg-KOH, to titrate a 1 g sample of crude oil. A higher crude oil acidity increases the magnitude of the negative charge in the oil/water interface, thus magnifying the difference in potential between the solid/water and water/oil interfaces. The higher potential difference between the two interfaces reduces the connate water film's stability. Consequently, the degree of oil-wetness is strongly proportional to the crude oil's acid number (Zhang and Austad, 2005).

2.3.3.2 Crude Oil Composition

Crude oils have complex and highly variable compositions that play a crucial role in determining their wetting properties. The components of a crude oil can be categorized under four main categories: saturates, aromatics, resins, and asphaltenes (SARA) in addition to nitrogen, sulfur, and oxygen compounds (NSO) and metal traces. The resins and asphaltenes are polar-bearing components that often contain the naphthenic and carboxylic acid groups. Skauge et al. (1999) have analyzed 12 different crude oil samples and found a direct correlation between the crude oil's asphaltene content and its acid content. However, asphaltenes themselves do not affect the carbonate wettability (Buckley, 1995; Standnes and Austad, 2003), but can strongly adsorb on clay minerals when present (Clementz, 1976; Collins and Melrose, 1983). Furthermore, Denekens et al. (1959) tested the tendency of fractioned oil to affect limestone wettability and found the nitrogenous surface-active compounds to have a significant oil-wetting effect.

2.3.3.3 Ionic Composition of Brine

The salinity of formation water can range from fresh water to extreme salinities that exceed 200 g/L. More importantly, the ionic composition of saline formation waters

is highly variable. Some ions, especially multivalent cations, can significantly affect the electrokinetic (zeta) potential of carbonates—these ions are called potential-determining ions (PDIs). The two primary PDIs in carbonate reservoirs are calcium (Ca^{2+}) and carbonate (CO_3^{2-}). Zhang and Austad (2005) and Strand et al. (2006) have demonstrated that sulfate ions (SO_4^{2-}) behave in an inverse way to calcium: an increase in the concentration of sulfates can reduce (or reverse) the oil-wetness of carbonates by adsorbing on calcite surfaces and changing the zeta potential to negative. On the other hand, magnesium ions (Mg^{2+}) have a similar effect to calcium ions in increasing the zeta potential of calcite at typical pH values of approximately 8. Furthermore, a reduction in the total ionic strength of the formation water can reduce the effect that each PDI can have on the zeta potential of calcite surfaces (Alroudhan et al., 2016), due to an increase in the size of the EDL at lower salinities.

2.3.3.4 Temperature

The effect of temperature on carbonate wettability is very complex since changes in reservoir temperature can significantly affect many rock-fluid and fluid-fluid interactions in addition to the relative volumes and thermophysical properties of reservoir fluids. The consequence of reservoir heating is a subject studied by multiple researchers in steam flooding (Rao, 1999), but will not be addressed in this present work since wettability alteration by chemical injection does not involve changes in reservoir temperature.

Over geologic timescales, the presence of calcium carbonate at higher temperatures can result in the decomposition of carboxylic acid groups—a process known as decarboxylation (Shimoyama and Johns, 1971), leading to a reduction in the acid content of carbonate reservoirs—a catalyst for oil wettability. In a laboratory setting,

a higher temperature can aid the process of aging a rock sample (Jadhunandan and Morrow, 1995; Zhou et al., 1995).

2.3.3.5 Reservoir Mineralogy

Although calcite is the dominant mineral, carbonate rocks are very heterogeneous and can be made up of highly variable mineralogic composition of different carbonate minerals such as ankerite ($\text{Ca(Fe,Mg,Mn)(CO}_3)_2$), dolomite ($\text{CaMg(CO}_3)_2$), and siderite (FeCO_3) in addition to quartz (SiO_2) and clay minerals (Barber and Reeder, 1990). Several authors studied the zeta potential of limestones (Chen et al., 2014; Alroudhan et al., 2016), chalk (Zhang and Austad, 2005; Strand et al., 2006), and dolomite (Alotaibi et al., 2011; Kasha et al., 2015), but research that decouples the impact of each mineral content on carbonates zeta potential is scarce. Therefore, to reduce the uncertainty and have more representativeness, the studied carbonates in this research are limestone outcrop and reservoir rocks of known and relatively similar mineralogy.

2.3.4 Oil Retention Mechanism

Rock-fluid interactions and specifically the rock's wettability affect the residual oil saturation (S_{or}) significantly. Ideally, intermediate-wet porous media with contact angles of slightly less than 90° correspond to the highest displacement efficiency, where the capillary pressure is positive and at its lowest magnitude (Morrow, 1979; Jadhunandan and Morrow, 1995). On the other hand, if the porous medium is strongly water-wet, oil can be primarily trapped by capillary instability that result on a "snap-off" event at pore constrictions (throats) leading to a loss of connectivity in the oleic phase (Wardlaw, 1982; Mohanty et al., 1987); the oil is then retained as ganglia. The entrapped oil saturation under such mechanism is higher when the pore body to pore throat ratio is

high. Nevertheless, the displacement efficiency from a strongly water-wet porous medium is higher than that of an oil-wet porous medium (Lefebvre du Prey, 1973). In an oil-wet porous medium, oil is retained by two primary mechanisms: (1) capillary entrapment and to a lesser extent (2) surface trapping—both mechanisms are discussed in further detail in the following subsections.

2.3.4.1 Capillary Entrapment

In addition to the applied pressure gradient, there are three primary forces acting in the reservoir during oil displacement by water: viscous, capillary, and gravity forces. The capillary forces are resistant forces that are responsible for oil entrapment in pore throats. On a curved oil/water interface, the capillary pressure is the pressure difference between the oil and water phases, which is given by the Young-Laplace equation (Anderson, 1987a) that relates the radii of curvature (r_1 and r_2) to the oil/water interfacial tension (σ_{ow}). In a capillary tube model, the expression can be re-written to incorporate the contact angle (Θ) of the interface through the water ($\cos \Theta$) given that both radii of curvature are equal to the tube's radius (r_t), i.e.

$$P_c = P_o - P_w = \sigma_{ow} \left(\frac{1}{r_1} + \frac{1}{r_2} \right) = \frac{2\sigma_{ow} \cos \theta}{r_t}$$

In oil-wet reservoirs, oil creates a contact angle greater than 90° on the rock surface. This results in a negative capillary pressure, which does not facilitate the imbibition of water into oil-bearing pores. The negative capillary pressure is especially critical in narrow pore throats and naturally fractured reservoirs. Narrow pore throats result in capillary pressures that are not only negative, but excessively high in magnitude. In addition, in naturally fractured reservoirs, the fractures represent the reservoir's flow capacity, while most of the storage capacity is retained in the matrix; a negative capillary

pressure would result in water channeling into the fracture without counter-currently imbibing into the matrix to displace the oil (Van Golf-Racht, 1982).

2.3.4.2 Surface Trapping

In addition to capillary entrapment, oil is retained in oil-wet reservoirs as continuous thin films in contact with the pore walls (Wardlaw, 1996). The amount of oil retained by surface trapping is proportional to the pore's surface area and degree of surface roughness (Hirasaki and Zhang, 2003).

2.3.5 The Effect of Wettability on Relative Permeability and Waterflood Efficiency

The effect of wettability on the relative permeability and waterflood efficiency is addressed under three assumptions: (1) two-phase flow of oil and water, (2) wetted porous media where either oil or water is the wetting phase, and (3) negligible viscous and buoyancy forces.

The relative permeability of one phase is its effective permeability at any given water saturation, relative to the porous medium's absolute permeability. The difference between the wetting and non-wetting phase relative permeabilities at any given saturation is largely influenced by its connectivity and spatial distribution. Initially, the non-wetting phase in a wetted reservoir occupies the center of the larger pores, while the wetting phase occupies the smaller pores and remains in contact with the grain surfaces through thin films in the larger pores to minimize the system's energy (Anderson, 1987b).

During water imbibition into oil-wet reservoirs, the behaviors of the relative permeability curves possess unique characteristics as a result of the distribution of each phase in the porous medium (Jennings, 1957; Craig, 1971). Firstly, the connate water saturation in oil-wet reservoirs is often lower (less than 15%) than that of water-wet

reservoirs (greater than 20-25%). Secondly, the water and oil relative permeability curves tend to cross over at a lower water saturation in oil-wet reservoirs (less than 50%) than in water-wet reservoirs (greater than 50%). Lastly, the end-point relative permeability to water is significantly higher in oil-wet reservoirs (greater than 50%) compared to water-wet reservoirs (less than 30%) as a result of the water flowing in the larger pores (Figure 2.2).

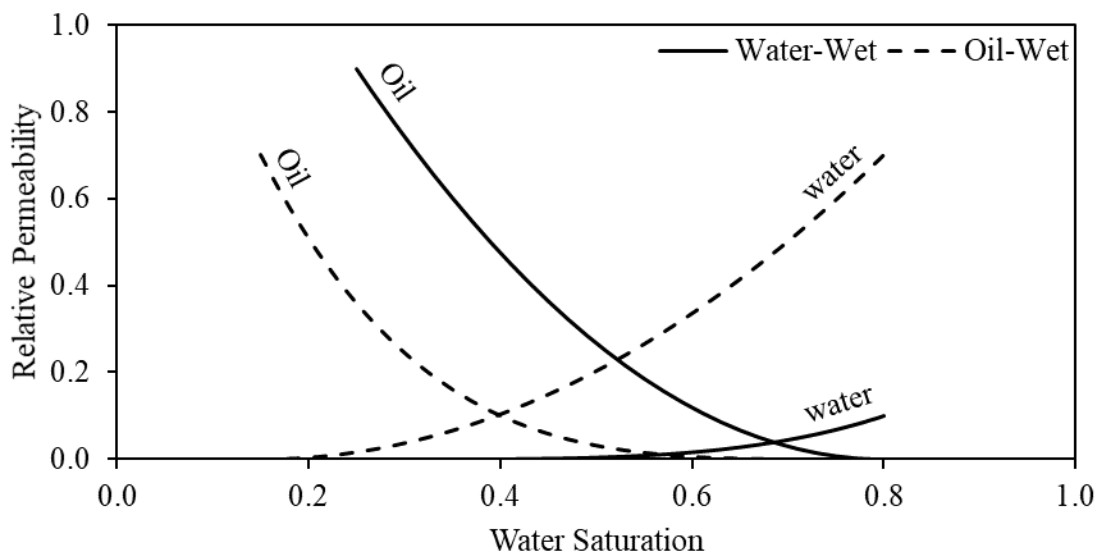


Figure 2.2 – Idealized schematic of the relative permeability behavior in oil-wet (dashed) and water-wet (solid) systems.

Due to the spatial distribution of each phase under oil-wet conditions and consequently the changes in relative permeability, waterflooding is significantly less efficient in oil-wet systems compared to water-wet systems (Anderson, 1987c). In water-wet systems oil is retained either as ganglia in the center of larger pores or as bypassed patches that are surrounded by water (Mattax and Kyte, 1961; Donaldson and Thomas, 1971). As a result, the oil phase is abruptly disconnected and becomes immobile. Thus, most of the oil is produced prior to the water breakthrough while the water/oil ratio

(WOR) increases rapidly afterwards (Owen and Archer, 1971). On the contrary, in oil-wet systems, water channels through the middle of the larger pores to displace the oil ahead of it (Raza et al., 1968), leading to a faster water breakthrough (Warren and Calhoun, 1955). As a result, the oil saturation and consequently the displacement efficiency at water breakthrough is significantly lower (Figure 2.3). As the waterflood progresses beyond the water breakthrough, oil will continue to be produced due to its phase connectivity as the WOR gradually increases over several pore volumes. Eventually, the waterflooding of oil-wet systems becomes uneconomical as significant amount of water need to be injected for every barrel of oil produced. This leads to a practical oil saturation (a remaining oil saturation that is not economically producible) that is lower than the true residual oil saturation.

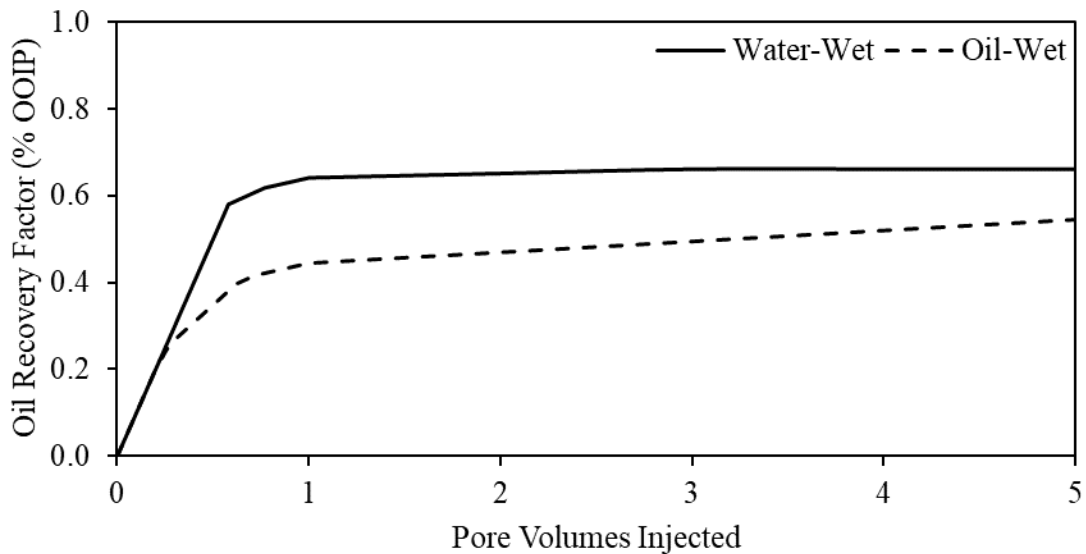


Figure 2.3 – Idealized schematic of the waterflood efficiency in oil-wet (dashed) and water-wet (solid) systems.

4. Zwitterionic or amphoteric: can potentially contain both positive and negative charges, e.g. betaines (Figure 2.7).

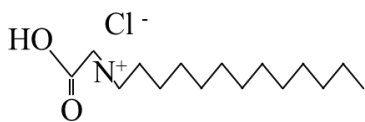


Figure 2.7 – The chemical structure of coco betaine (CB).

On the other hand, the hydrophobic tail group, often composed of hydrocarbons, provides the source of variability in the surfactant composition. The tail group can have a variable structure (linear, branched, or aromatic) in addition to incorporating a different number of carbon atoms, thus allowing for flexible chain lengths and structures (Green and Willhite, 1998).

2.4.1.1 Interfacial Tension

Surfactants are primarily used for their capability to reduce the interfacial tension—the work per unit area required to increase the interfacial area between two immiscible phases. In a system that consists of an aqueous phase and an oleic phase, the presence of surfactants in the aqueous solvent results in a higher thermodynamic free energy, leading surfactant molecules to preferentially move to the oil-water interface to reduce the system's free energy. At relatively low surfactant concentrations, surfactant monomers tend to especially orient in a manner that reduces the free energy of the system: the hydrophilic head group aligns towards the aqueous phase while the hydrophobic tail group aligns towards the oleic phase (Myers, 2006).

2.4.1.2 Critical Micelle Concentration (CMC)

At higher surfactant concentrations, where the oil-water interface is fully packed with surfactant monomers, the remaining dispersed molecules in the bulk solution tend to aggregate into micelles. In aqueous solvents, individual molecules in the micelle orient such that the hydrophilic head groups are aligned toward the outer boundary, shielding the hydrophobic tail groups from water. The critical micelle concentration (CMC) of a surfactant describes the onset of aggregation—the concentration above which surfactant monomers form aggregates (Figure 2.8).

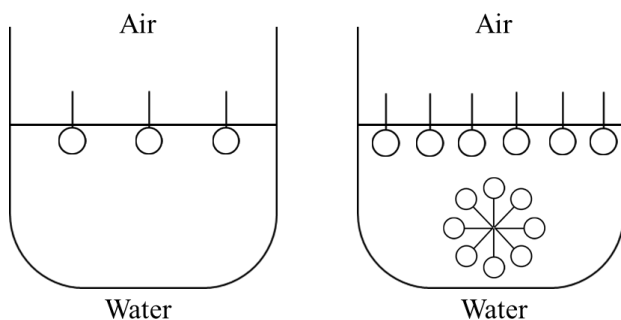


Figure 2.8 – Comparison of a surfactant solution below (left) and above (right) the CMC.

Figure 2.9 shows an idealized schematic of the relationship between a surfactant's surface tension and its concentration. At extremely low concentrations, the surface tension of the solutions is similar to that of water (~ 72 mN/m). As the surfactant concentration increases, the surface tension declines linearly on a semi-log scale. The lower rate of change in the surface tension of surfactant B as opposed to the sharp decline in surfactant A is indicative of the presence of different chemical mixtures in the former's composition. At the CMC (0.02 wt% for surfactant A and 0.15 wt% for surfactant B), all the additional surfactant monomers form aggregates in the bulk solution, thus not impacting the surface tension. The CMC of a surfactant solution has very important

economic implications; surfactant B must be used at nearly 10 times the concentration of surfactant A to achieve the lowest possible surface tension. The technical implication of the CMC will be addressed at a later section when describing the wettability alteration mechanism.

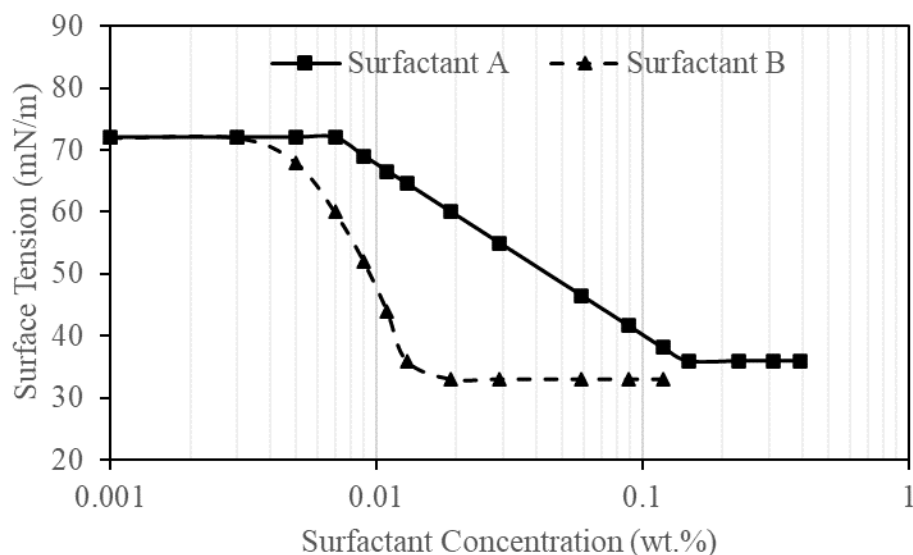


Figure 2.9 – Idealized schematic of a surfactant’s CMC determination.

2.4.1.3 The Effect of Surfactant Structure

The structure of each surfactant plays an important role in determining its viability for achieving the desired objective. One important surfactant characteristic is the hydrophile-lipophile balance (HLB), which is an arbitrary number that ranges from 1-20 that describes the surfactant’s emulsification effectiveness (Myers, 2006). At the upper end of the scale, the surfactant is more hydrophilic, whereas the lower end surfactants are more lipophilic. Control of the surfactant’s lipophilicity is typically achieved proportionally by the length of the hydrocarbon chain (del Rio et al., 1995)—a lower HLB value can result in surfactants that can easily partition in the oleic phase. Surfactant partitioning is described by the partitioning coefficient (K): the ratio of surfactant

concentration in the oleic phase (C_{oil}) relative to its concentration in the aqueous phase (C_{water}), i.e.

$$K = \frac{C_{oil}}{C_{water}}$$

Furthermore, surfactants are sensitive to the system's temperature; in lieu of micellization, the surfactant molecules reduce the system's free energy by forming unfavorable aggregates that are not thermodynamically stable in the bulk solution when used in harsh conditions. A surfactant solution may appear murky when used at temperatures that exceeds its cloud point (CP)—the temperature above which surfactants form cloud-resembling solid suspensions. The CP is more detrimental to nonionic surfactants, hence their application at harsh temperatures is challenging; nonetheless, the CP can also limit the use of some cationic and anionic surfactants (Nakama, 1990). Longer hydrocarbon chain lengths can increase the surfactant's tolerance to harsh reservoir temperatures (Solairaj et al., 2012).

On the other hand, the Krafft temperature of a surfactant describes the minimum temperature requirement for the surfactant monomers to form micelles. Longer hydrocarbon chain lengths with low HLB values typically cause a lower surfactant solubility in the aqueous phase, which in turn result in higher Krafft temperatures (del Rio et al., 1995; Chu and Feng, 2011). In high-temperature applications, the cloud point is typically the limiting factor in chemical selection rather than the Krafft temperature.

In addition to the temperature, the aqueous phase pH, ionic strength, and composition significantly impact the aqueous stability of surfactants. The biggest limiting factor in chemical selection is the aqueous phase hardness, which often result in surfactant phase separation through gel formation, crystallization, or precipitation as a result of the surfactant's incompatibility with the aqueous phase composition. Anionic

surfactants, especially sulfonates, are more prone to precipitation in hard brines due to the interaction between their negative charge and the positive charge of multivalent cations (Nelson, 1981; Hirasaki and Zhang, 2003; Gupta et al., 2009). One way to mitigate the presence of divalent cations is through using sequestration agents such as alkali anions (Holm and Robertson, 1981), sodium metaborate (Flaaten, 2008; Zhang, 2008), and ethylene diamine tetraacetic acid (EDTA) or sodium polyacrylate (NaPA) (Chen and Mohanty, 2013).

In addition, the surfactant's tolerance to the presence of divalent cations can be enhanced through ethoxylation—a process by which ethylene oxides (EO) are incorporated in the surfactant structure (Hirasaki et al., 2008). On the other hand, propoxylation, i.e. the addition of propylene oxide (PO) groups reduces the surfactant's tolerance to salinity. However, the hydrophobicity of the PO groups increases the solubilization ratio of oil, thereby reducing the interfacial tension. The balance between EO and PO groups is a classical low-cost optimization process, in lieu of using costly alkalis or co-surfactants, to ensure the surfactant's tolerance to harsh reservoir conditions while maintaining the breadth and magnitude of the desired low interfacial tension (Bourrel and Schechter, 1988; Aoudia et al., 1995; Levitt et al., 2006).

The length and structure of the hydrophobic tail group exerts a large influence on the microemulsion phase behavior. Straight long chains promote oil-in-water microemulsion, while branched tails promote water-in-oil microemulsion (Barnes et al., 2012). Furthermore, the surfactant's adsorption in porous media, while largely influenced by the charge of the head group, is also proportional to its hydrophobicity—branched hydrophobic tails with increasing number of PO groups result in a higher adsorption, while straight hydrocarbon chains have the opposite effect (Wilson et al., 2019).

The charge of the hydrophilic group is also crucial in determining the surfactant retention, and as a result, the economic viability of the micellar flooding project. The surfactant retention is generally a combination of (1) adsorption and (2) partitioning in immobile oleic phase. Anionic surfactants have a higher capacity to adsorb onto carbonate surfaces due to the potential difference between anionic head groups and cationic carbonate surface. On the other hand, cationic surfactants have the lowest adsorption tendency due to charge similarities. Zwitterionic surfactants also do not greatly adsorb on carbonates, especially at higher temperatures and salinities (Nieto-Alvarez et al., 2012).

2.4.2 Surfactant Application in EOR I: Wettability Alteration

Significant research has been devoted to wettability alteration since wettability is the most important controllable factor in determining the waterflood efficiency and the economically achievable (practical) residual oil saturations. The efforts ranged from modifications to the injected water ionic composition, pH, in-situ saponification through alkalis in addition to the use of surfactants. All these methods are geared to ultimately alter the porous media's wettability to a more favorable water-wet state, thus promoting water imbibition into oil-bearing pores.

Most research on wettability alteration through surfactants was devoted to sandstone reservoirs, primarily due to the high divalent cations concentration in carbonate reservoirs, which results in limited chemicals compatibility. Furthermore, the positively charged carbonate surfaces result in a higher surfactant retention of the most commonly used anionic surfactants. Yet, carbonates are more likely to be oil-wet as discussed earlier, making wettability alteration in carbonates a more pressing need.

Despite the limitations of high temperature, low permeability, and high hardness, surfactants have successfully been used in a laboratory setting to alter the wettability of low-permeability chalk (Austad and Standnes, 2003; Zhang and Austad, 2005), high-hardness carbonates (Seethepali et al., 2004; Xie et al., 2005) high-temperature and high-salinity carbonates (Gupta and Mohanty, 2008; Chen and Mohanty, 2014). Full field applications of wettability alteration through surfactant flooding are scarce, but examples of successful pilot tests and single-well treatments can be found in the Yates (Chen et al., 2000) and the Cottonwood Creek (Weiss et al., 2004) fields, respectively.

2.4.2.1 Wettability Alteration Mechanisms

Three primary mechanisms have been proposed for the surfactants role in altering the rock matrix wettability, dependent on the crude oil composition, rock mineralogy, surfactant functionality, and ionic composition of the brine: surfactant adsorption, ion-pair formation, and micellar solubilization of organic components.

Firstly, the rock surface's wettability is altered by surfactant adsorption, mostly through anionic surfactants. Oil-wet surfaces are hydrophobic; as a result, the hydrophobic tails of surfactant monomers tend to be attracted to and eventually adsorb onto such surfaces, leaving the hydrophilic heads exposed. The newly formed hydrophilic bi-layer causes a change in the rock surface's wettability from oil-wet to water-wet (Spinler and Baldwin, 2000). However, this type of surfactant interaction with the rock-surface is (1) reversible and can cause oil re-imbibition (Chen et al., 2000) and (2) does not mobilize the oil that is surface-trapped since it is essentially masked.

A second wettability alteration mechanism is pertinent to the ionic interaction between the surfactant's hydrophilic head group and the adsorbed carboxylic acids, mostly through cationic surfactants. The differences in charge between cationic

surfactants and carboxylic acids results in the formation of ion-pairs that essentially desorb these oil-wetting components from the rock's surface (Austad and Standnes, 2003). The desorption of oil from the rock's surface through ion-pair formation is irreversible and results in the alteration of the rock's surface from oil-wet to preferentially water-wet. The ion-pair is not soluble in the aqueous phase but is rather solubilized in the oleic phase or in micelles.

The third wettability alteration mechanism proposed by Kumar et al. (2008) is the micellar solubilization of adsorbed organic components. A surfactant solution that is in contact with an oil film will solubilize the oil-wetting molecules in micelles, slowly desorbing or “peeling off” these components to alter the rock's surface from oil-wet to preferentially water-wet. The mechanism by which zwitterionic surfactants alter the wettability of carbonates is not fully understood due to their high cost and relatively recent development in wettability alteration.

2.4.2.2 Spontaneous Imbibition

Spontaneous imbibition is the displacement of the nonwetting fluid by the wetting fluid in a porous medium by capillary action (Morrow and Mason, 2001) or gravity drainage (Schechter et al., 1994). The evaluated surfactants in this research are of a relatively high IFT in the range of 1 mN/m; therefore, gravity-aided water imbibition is deemed negligible.

In a laboratory setting, the water imbibition into oil-wet rock samples is initially delayed (Morrow and Mason, 2001). This delay, or induction time, is an experimental artifact that results from the adsorption of organic matter on the outer surfaces of rock samples. Capillary-induced water imbibition into core plugs is proportional to the square root of time (Washburn, 1921), while the experimental results are scaled by a

dimensionless time (t_D) that incorporates the time (t), porosity (ϕ), permeability (k), interfacial tension (σ), wetting and non-wetting fluid viscosities (μ_w , μ_{nw}), and characteristic length (L_c), where the characteristic length is a function of the sample's length (L) and diameter (D) (Ma et al., 1997):

$$t_D = t \frac{1}{L_c^2} \sqrt{\frac{k}{\phi} \frac{\sigma}{\mu_w \mu_{nw}}}$$

$$L_c = \frac{L \times D}{\sqrt{D^2 + 2L^2}}$$

2.4.3 Surfactant Application in EOR II: Ultra Low IFT Micellar Flooding

The subject of ultra low IFT micellar flooding will not be addressed in detail since the surfactants encountered in this research have relatively high IFTs in the order of 1 mN/m. Nonetheless, these IFTs are approximately an order of magnitude lower than typical crude-oil/brine IFTs of 20-30 mN/m (Hirasaki et al., 2008); therefore, the reduction of IFT will have a secondary effect to wettability alteration.

In addition to the effect of wettability alteration, the interfacial tension between the displacing (water) and displaced (oil) fluids play an important role in determining the magnitude of the residual displaced phase saturation by reducing the capillary pressure and promoting the onset of oil mobilization. The effect of capillary pressure is represented through the capillary number, a dimensionless number that describes the ratio between viscous to capillary forces (Brownell and Katz, 1947; Chatzis and Morrow, 1981) in terms of permeability (k), potential gradient ($\Delta P/L$), and oil/water interfacial tension (σ). A variable expression of the capillary number (Moore and Slobod, 1956; Taber, 1969) incorporates the effect of the reservoir's wettability ($\cos \Theta$) where v is the interstitial velocity and μ_w is the water viscosity:

$$N_c = \frac{k \nabla \phi}{\sigma_{ow}} \approx \frac{k \Delta P}{\sigma_{ow} L} \approx \frac{v \mu_w}{\sigma_{ow} \cos \theta}$$

The impact of the capillary number on the ROS is typically modeled in a capillary desaturation curve (CDC)—a curve that describes the ROS as a function of N_c . Chatzis and Morrow (1981) studied the impact of capillary number on sandstones, where the onset of ROS reduction occurs at a critical capillary number in the magnitude of approximately 10^{-4} ; beyond the critical capillary number, the ROS is sharply reduced. The effect of capillary number is especially important in carbonate reservoirs where the CDC possess a different behavior. Due to the rocks' heterogeneity and wide and multimodal pore size distributions, the CDC of carbonates does not exhibit a critical capillary number but rather continuously declines as the capillary number is increased (Kamath et al., 2001).

CHAPTER 3 MATERIALS AND PROCEDURES

3.1 MATERIALS

This section describes the materials used in this research.

3.1.1 Crude Oil

The crude oil is a 40° API light oil with a density of 0.83 g/cm³. At the reservoir temperature of 116 °C, the live oil viscosity is 0.44 cp. The oil contains approximately 10 wt% wax and less than 1 wt% asphaltenes with a pour point of 30 °C. Its detailed composition was determined by SARA analysis, while the acid and base content was characterized using the ATSM 664-89 method.

3.1.2 Surfactants

A total of 20 different surfactants were used in this research: 5 cationic surfactants, 6 anionic surfactants, 8 nonionic surfactants, and 1 amphoteric (zwitterionic) surfactant (Table 3.1). The surfactants were selected based on their commercial availability, tension, charge of head group, length of hydrophobic tail, predicted tolerance to hardness, and historical performance in wettability alteration. The surfactants were used as single-system surfactants, i.e. no attempt was made to use a combination of two or more surfactants in the same solution.

Table 3.1 – Surfactants used for wettability alteration.

Surfactant	Classification	Provider
CTAC	Cationic	Sigma Aldrich
BTC [®] 8358	Cationic	Stepan
Ethoquad [®] 0/12 PG	Cationic	Nouryon
Stepanquat [®] 3712-W	Cationic	Stepan
Benzalkonium Chloride	Cationic	Alfa Aesar
Soloterra [®] G4-12	Anionic	Sasol
Calfax [®] 16-35	Anionic	Pilot
Calimulse [®] PR	Anionic	Pilot
Enordet [®] O332	Anionic	Shell Chemicals
Dowfax [®] 3B-2	Anionic	Dow Chemical
Calfax [®] DB-45	Anionic	Pilot
ASPIRO [®] S-2430x	Nonionic	BASF
Butyl Diglycol	Nonionic	Sigma Aldrich
Phenol 2PO-60EO	Nonionic	Harcros Chemicals
Phenol 2PO-70EO	Nonionic	Harcros Chemicals
2EH-2PO-50EO	Nonionic	Harcros Chemicals
2EH-2PO-60EO	Nonionic	Harcros Chemicals
Tergitol [®] NP-10	Nonionic	Dow Chemical
ASPIRO [®] S-2410	Nonionic	BASF
Mackam [®] CB-35	Amphoteric	Solvay Novecare

3.1.3 Salts and Additives

Reagent grade salts sodium chloride, calcium chloride dihydrate, magnesium chloride hexahydrate, and sodium sulfate were purchased from Fisher Scientific with a purity greater than 99%. The salts were used as purchased.

3.1.4 Carbonate Rocks

The carbonate samples used in this research are outcrop rocks and reservoir rocks. The outcrop (Edwards Yellow Limestone) was selected based on its similarity to the mineralogy and petrophysical properties of the reservoir rock. The mineralogy of both rocks was determined through an X-ray diffraction (XRD) test, which was conducted by Premier Oilfield Group. The pore size distribution of both rock types was determined through a mercury injection capillary pressure (MICP) test after Soxhlet extraction.

3.2 PROCEDURES

This section describes the testing procedures conducted in this research.

3.2.1 Brine Preparation

Synthetic seawater was prepared in 4 L batches by mixing deionized water with a minimum resistivity of 17 M Ω -m with sodium chloride (NaCl), calcium chloride dihydrate (CaCl₂·2H₂O), magnesium chloride hexahydrate (MgCl₂·6H₂O), and sodium sulfate (Na₂SO₄). The brine was then filtered with 0.45 μ m cellulose filter paper in a vacuum filtration flask before use to prevent pore plugging.

3.2.1.1 Total Dissolved Solids Measurement

The total dissolved solids (TDS) was measured after mixing every batch with a Milwaukee Instruments® MA871 Digital Brix Refractometer to ensure the relative

accuracy of brine preparation. The refractometer was calibrated and cleaned with deionized water before use.

3.2.1.2 pH Measurement

The pH of brine batches was measured with a Thomas Scientific Orion[®] 5 Star digital pH meter. The electrode was thoroughly washed with deionized water and the meter was calibrated before use in three buffer solutions with pH values of 7, 4, and 10, respectively.

3.2.2 Crude Oil Preparation

The crude oil was filtered in 400 ml batches through a 0.5 μm in-line stainless steel filter under 100 psi air pressure gradient to remove solid contaminants that could result in pore plugging. The filtration was conducted at 70 °C to avoid wax or asphaltene dropout. During the experiments that were conducted at room temperature, the oil was mixed with 20 wt% toluene to mimic the live crude oil properties. The reservoir-temperature experiments were conducted on dead crude oil.

3.2.2.1 Viscosity Measurement

The dead oil viscosity was measured with a TA[®] Instruments Discovery Hybrid Rheometer (DHR-3[®]).

3.2.3 Surfactant Solutions Preparation

The surfactant stock solutions were prepared at the desired surfactant concentrations. The surfactants were mixed with the synthetic seawater based on each surfactant's respective activity. The solutions were then filtered with 0.45 μm cellulose filter paper in a vacuum filtration flask prior to use to prevent possible pore plugging.

3.2.4 Carbonate Discs Preparation

An outcrop core with 1.5-inch diameter was oven dried at reservoir temperature for 24 hours, then sliced into discs of 0.2-inch thickness (Figure 3.1). The Discs were polished with Crystal Master[®] polisher from both sides to reduce their surface roughness.



Figure 3.1 – A sample of the outcrop carbonate discs used for wettability screening.

3.2.4.1 Carbonate Discs Aging

The discs were washed and equilibrated in synthetic seawater for 24 hours at reservoir temperature, then placed in a high-temperature glass container filled with crude oil and aged for two weeks at reservoir temperature to alter their wettability to oil-wet.

3.2.5 Initial Screening

The methodology to screen surfactants for their efficacy at altering carbonates wettability is described in this section.

3.2.5.1 Aqueous Stability Testing

The aqueous stability of all 20 surfactants was tested with 0.5 wt% solutions in synthetic seawater for three days at 116 °C to evaluate the surfactants tolerance to temperature and hardness. The test solutions were monitored for precipitation, gel formation, and cloud point, which indicate aqueous instability at reservoir conditions.

3.2.5.2 CMC Determination

The critical micelle concentration of all aqueous stable surfactants was determined by preparing 4 wt% stock solutions and measuring the surface tension of each surfactant at a series of dilute concentrations. The surface tension was measured at room temperature and plotted as a function of surfactant concentration on a semi-log scale. The CMC was determined at the concentration beyond which no significant change in surface tension occurs. The measurements were conducted on Ramé-Hart® model 500-F1 tensiometer, which consist of a light source, camera, stand, and fluid dispenser. The fluid dispenser is thoroughly cleaned with deionized water before testing a new surfactant and with every change in concentration. For every surfactant, the surface tension was measured in ascending order of concentrations (i.e. from the lowest to the highest concentrations) to avoid possible contamination resulting from cleaning errors. The surface tension measurements are conducted using the pendant drop method and analyzed by the software using the Young-Laplace equation.

3.2.5.3 Wettability Screening

An oil-wet carbonate disc was placed in a high-temperature glass container that contains synthetic seawater at reservoir temperature. Changes on the disc were monitored for 10 days to establish a baseline for the wettability of this control sample.

Similarly, different oil-wet carbonate discs were placed in bottles containing the aqueous stable surfactant solutions in similar testing conditions and monitored for a similar period. The surfactant solutions were tested at a concentration at least four times their respective CMC. Pictures were taken at different time intervals and the water-advancing contact angle on top of each disc was estimated with an on-screen protractor. Additionally, observations were noted about the shape of oil droplets, size of oil droplets,

color changes in the carbonate disc, and degree of oil solubilization in the aqueous phase. The surfactants that did not show promising potential for wettability alteration were eliminated.

3.2.6 Contact Angle Measurement

The final wettability of the carbonate discs was quantified by measuring the water-receding contact angle of the control sample in addition to the samples that showed promising results during the wettability screening. The measurements were conducted on a Ramé-Hart® model 500-F1 goniometer, where an oil droplet was introduced through an inverted capillary tube to the bottom of each disc, immersed in its respective test solution at room temperature, and allowed to equilibrate until no significant change in contact angle was observed. A minimum of five measurements were taken to evaluate the mean and standard deviation of the contact angle measurements.

3.2.7 Interfacial Tension Measurement

The surfactants that altered the carbonate disc's wettability to water-wet or intermediate-wet were equilibrated with crude oil at reservoir temperature for three days. The surfactant solutions were prepared at a concentration that is consistent with the planned spontaneous imbibition experiment. After equilibration, the oil-water interfacial tension of each system was measured with a Krüss® Spinning Drop Tensiometer (SDT). The measurements were conducted at 100 °C due to the temperature limitation of the instrument.

3.2.8 Spontaneous Imbibition

The surfactants that altered the wettability of the carbonate discs to water-wet or intermediate-wet state were selected for further evaluation through spontaneous imbibition experiments—first on outcrop core plugs, and then on reservoir core plugs.

3.2.8.1 Spontaneous Imbibition Apparatus

The spontaneous imbibition cells were fabricated in the glass shop at the University of Texas at Austin Department of Chemistry (Figure 3.2). The cells consist of a bottom Teflon bushing. A groove of 1.5-inch diameter and 0.25-inch depth was drilled in the bushing at the machine shop in the Department of Petroleum and Geosystems Engineering at the University of Texas at Austin. The groove helps stabilize the plugs from tilting and contact with the sides of the glass cell during transport. Before seating the plugs, the groove was filled with glass beads to allow the imbibing solution access to the bottom of the core plugs. The top of the imbibition cell has a relief valve that prevents the aqueous solution from evaporation while ensuring the safety of the apparatus. The neck of the cell is graduated to allow for oil drainage measurements. Before the experiments, the cells were filled with deionized water and placed in the oven in similar testing conditions to accurately measure and correct for the water expansion factor.

A core plug was placed in each cell, surrounded by its test solution. The oil recovery rate was monitored for over six months, while noting changes to the surface of the plug and the behavior of oil drainage. The tests were conducted in an 80 °C oven due to the temperature rating of the apparatus.



Figure 3.2 – The spontaneous imbibition apparatus.

3.2.8.2 Outcrop Core Plugs Preparation

Two outcrop cores were oven dried at reservoir temperature for 24 hours. The cores were then wrapped with a heat shrink wrap and vacuumed to at least -14.2 psi before being fully saturated with crude oil and aged for one month. Each core was then sliced with electric powered core saw to four plugs of equal length. The porosity of each plug was estimated from the core's porosity and the plug-to-core mass ratio. Each plug's permeability was assumed equal to the core it was cut from.

3.2.8.3 Core Plug Cleaving

At the end of the spontaneous imbibition experiments, each core plug was axially cleaved through the center with an electric powered core saw to understand the mechanism of water imbibition and the distribution of the remaining oil.

3.2.8.4 Reservoir Core Plugs Preparation

A reservoir composite core made of four plugs separated by 3-micron cellulose filter paper was wrapped with a heat shrink wrap, then cleaned with 2 PV toluene, 2 PV isopropyl alcohol, and 2 PV methanol in succession. Afterwards, the core was oven dried at reservoir temperature for 24 hours, then vacuumed to at least -14.2 psi before being fully saturated with crude oil and aged for one month. Three of the four core plugs were selected for spontaneous imbibition experiments; the plugs were selected based on their physical and petrophysical similarity. The three spontaneous imbibition experiments contained a control sample in addition to the top two performing surfactants in the outcrop spontaneous imbibition experiment.

3.2.9 Core Floods

The core flooding equipment and procedures are detailed in this section.

3.2.9.1 Core Holder

A cylindrical stainless steel core holder was used for the core flooding experiment. The core holder contains a cylindrical rubber sleeve that creates two isolated annuli. The inner annulus contains the core, while the outer annulus is filled with deionized water and pressurized to a confining pressure of 1,000 psi to create a compressive force on the core. Both ends of the core holder are closed with a metal cap sealed with two O-rings. The caps have a fluid distributor at both ends that is tightly secured against the core with a safety pin. The core holder was initially equipped with a dummy core and subjected to pressurized air to test for leaks in the sleeve, connections, fittings, or O-rings.

3.2.9.2 Accumulators

Three stainless steel accumulators were used for fluid injection. The first accumulator was used for oil injection with a capacity of 750 ml, the second accumulator was used for water injection with a capacity of 500 ml, and the third accumulator was used for surfactant injection with a capacity of 350 ml. All three accumulators contain a cylindrical piston—the injected fluid is placed above the piston, while the piston is pushed with mineral oil from the bottom side. The piston is equipped with O-ring that seals the injected fluid from the mineral oil. Both ends are closed with a metal cap and sealed with O-rings to prevent fluid leaks and maintain the desired pressure inside the accumulators.

3.2.9.3 Pumps

Two pumps are used in the core flooding experiment. Both pumps are Quizix® Qx Series Precision Pumps provided by Chandler Engineering, which operate with two independent motor-drive pistons. The first pump is connected to a deionized water source and is used to supply the required confining pressure in the core holder. The second pump is connected to a mineral oil source that is used for injection into the stainless-steel accumulators. The pumps are operated on a constant bidirectional pressure or a constant rate delivery mode, based on need.

3.2.9.4 Pressure Transducers

The inlet and outlet of the core holder are connected to pressure transducers with polyether ether ketone lines (PEEK). The lines are flushed with deionized water before the core flood to eliminate trapped gas. The pressure transducers measure the whole pressure drop across the core and transmit the electric signal to a data acquisition station.

The pressure drops are plotted in real time at the data acquisition station by NI Labview® software at a frequency of 1,000 Hz and recorded every 30 seconds.

3.2.9.5 Fraction Collectors

ISCO Retriever® 500 fraction collector is used to collect the core flood effluent. The fraction collector is equipped with 15-ml graduated test tubes and can be programmed to switch from one tube to the next by an automatic timer. The fraction collector was programmed to switch after collecting 5 ml of effluent.

3.2.9.6 Core Preparation

One outcrop core was used for core flooding experiment. The outcrop core was oven-dried for 24 hours, then its dimensions and dry mass were measured. The core was then wrapped with a heat shrink wrap and vacuumed in a core holder under 1,000 psi confining pressure to at least -14.2 psi. The vacuuming process was conducted by alternating CO₂ injection and vacuuming for at least three cycles to ensure no trapped immiscible gas is present inside the core.

3.2.9.7 Core Flood Setup

The core flood was conducted on two adjacent ovens (Figure 3.3). The first oven is set at reservoir temperature of 116 °C and contains the core holder and the accumulator. The second oven contains the fraction collector and is set at 45 °C due to the temperature limitation of the fraction collector. The end of the effluent line is equipped with a back-pressure regulator (BPR) set at 100 psi to prevent the effluent from evaporation. The effluent line connecting both ovens is insulated with cardboard and aluminum foil to reduce heat loss.

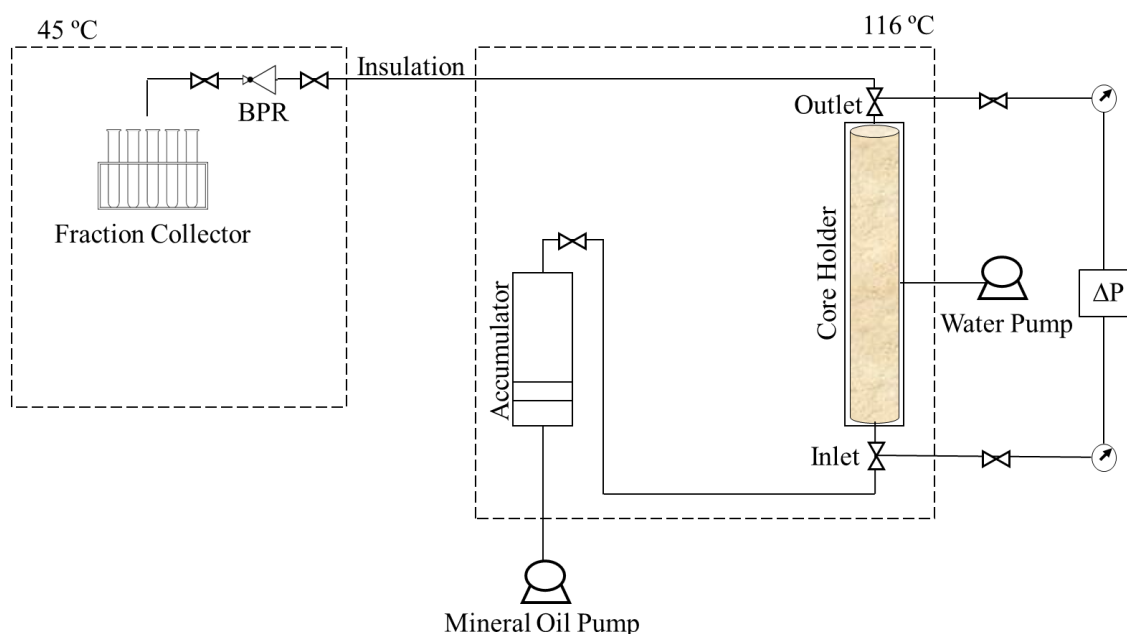


Figure 3.3 – Core flooding setup

3.2.9.8 Oil Flooding

The core holder containing a core under vacuum and the accumulator containing filtered dead oil are placed in the first oven at 70 °C and allowed to reach thermal equilibrium. Then, the accumulator containing crude oil and the metal line upstream of the core holder are pressurized to 200 psi under constant bidirectional pressure using mineral oil, while the core holder inlet valve is closed. The pump initial volume is then recorded. Afterwards, the core inlet is opened to allow oil to fully saturate the evacuated core. After 24 hours, the final pump volume is recorded. The core's effective porosity is calculated as the difference between the initial and final pump volumes (i.e. the volume of mineral oil used to displace the piston).

After oil saturation, the pump connected to the oil accumulator is switched to constant rate delivery and the core is flooded with oil, while opening the outlet valve. The

pressure drop corresponding to the injection rate is recorded via the pressure transducers. The pressure drop is considered stable if the pressure doesn't change by more than 1 psi over a 2-minute interval. Three different measurements are taken at the injection rates of 1.00 ml/min, 0.75 ml/min, and 0.50 ml/min. The permeability of each step is calculated using Darcy's law. The absolute permeability is calculated as the arithmetic average of all three measurements.

3.2.9.9 Core Aging

After measuring the absolute permeability, the temperature of the oven is increased to 116 °C to age the core at reservoir conditions. The core is kept under these aging conditions for 1 month. Afterwards, the oil inside the core is refreshed by injecting 2 PV of unused dead crude oil.

3.2.9.10 Waterflooding

The oil accumulator in the first oven is replaced with the second accumulator containing seawater filtered with 0.45-micron cellulose filter. After reaching thermal equilibrium, the core is flooded with 2 PV of seawater at an interstitial velocity of approximately 0.5 ft./day.

3.2.9.11 Surfactant Flooding

The water accumulator in the first oven is replaced with the third accumulator containing 1 wt% surfactant solution, filtered with 0.45-micron cellulose filter. After reaching thermal equilibrium, the surfactant solution is injected at a similar interstitial velocity to water flooding (0.5 ft./day); the volume of injected surfactant solution is equal to the final aqueous phase volume after the waterflood. Both the core inlet and outlet are

then closed to allow the surfactant to soak inside the core. Afterwards, the surfactant solution injection is resumed to evaluate changes in the residual oil saturation.

3.2.9.12 Effluent Analysis

The effluent test tubes are centrifuged for 10 minutes, then the oil-cut and water-cut are measured. For samples containing water, the pH of the aqueous phase is measured using a similar procedure to the one described in section 3.2.1.2 after separating the aqueous phase from the oleic phase. The surfactant concentration in the effluent was not measured, but the samples were retained for future measurement.

3.3 CALCULATIONS

3.3.1 Spontaneous Imbibition Calculations

3.3.1.1 Plugs Pore Volume

The porosity of each plug is estimated by dividing the difference in its saturated (m_s) and dry mass (m_d) by the oil density (ρ_o).

$$PV = \frac{m_s - m_d}{\rho_o}$$

3.3.1.2 Oil Recovery Factor

The oil recovery factor (RF) is calculated by dividing the recovered oil volume (V_r) by the plug's pore volume (V_p) since all the plugs are 100% saturated with oil.

$$RF = \frac{V_r}{V_p}$$

3.3.1.3 Time-Scaling

The non-dimensional time of spontaneous imbibition is scaled using the equation proposed by Ma et al. (1997). First, the plug's characteristic length (L_c) is calculated, where L and D are the plug's measured length and diameter.

$$L_c = \frac{L \times D}{\sqrt{D^2 + 2L^2}}$$

Then, the dimensionless time (t_D) is calculated using the time (t), porosity (ϕ), permeability (k), interfacial tension (σ), wetting and non-wetting fluid viscosities (μ_w , μ_{nw}), and characteristic length (L_c).

$$t_D = t \frac{1}{L_c^2} \sqrt{\frac{k}{\phi} \frac{\sigma}{\mu_w \mu_{nw}}}$$

3.3.2 Core Flood Calculations

3.3.2.1 Physical Properties

The diameter (d) of the core is calculated as the arithmetic average of three different measurements at the top, center, and bottom of the core. Similarly, the length (L) of the core is arithmetic average of three different measurements: one through its center and two through its edges. The bulk volume (V_b) is calculated through the cylindrical volume formula using the average values of diameter and length.

$$V_b = \frac{\pi}{4} d^2 L$$

3.3.2.2 Effective Porosity

The core's effective pore volume (V_p) is calculated from the volume of mineral oil required to displace an equivalent volume of crude oil from the accumulator to the core holder (ΔV_{pump}) less the dead volume in the connecting line (V_{dead}). Subsequently,

the core's effective porosity (ϕ_e) is then calculated by dividing its pore volume by its bulk volume.

$$V_p = \Delta V_{pump} - V_{dead}$$

$$\phi_e = \frac{V_p}{V_b}$$

3.3.2.3 Effective Permeability

The effective permeability (k_e) of the core is calculated using Darcy's law after measuring the pressure drop across the core (ΔP), where q is the constant injection rate, μ is the fluid viscosity at the testing temperature, A is the core's average cross sectional area, and L is the core's average length.

$$k_e = \frac{q \mu}{A} \cdot \frac{L}{\Delta P}$$

3.3.2.4 Phase Saturation

The remaining oil volume (V_{oil}) is calculated by subtracting the recovered oil volume (V_{or}) from the initial oil volume (V_{oi}). Subsequently, the oil saturation is calculated by dividing the remaining oil volume by the core's pore volume (V_p).

$$V_{oil} = V_{oi} - V_{or}$$

$$S_o = \frac{V_{oil}}{V_p}$$

$$S_w = 1 - S_o$$

3.3.2.5 End-Point Relative Permeability

The end-point water permeability (k_w) is calculated through Darcy's law using the constant water injection rate (q_w), steady-state pressure drop (ΔP_{ss}), water viscosity (μ_w), and the core's length (L) and cross-sectional area (A). The end-point water relative

permeability (k_{rw}°) is then calculated by dividing the water permeability by the core's effective permeability.

$$k_w = \frac{q_w \mu_w}{A} \cdot \frac{L}{\Delta P_{ss}}$$

$$k_{rw}^\circ = \frac{k_w}{k_e}$$

3.3.2.6 Effluent Composition

The oil cut (f_o) and water cut (f_w) of the effluent are calculated by dividing the recovered phase volume (V_o and V_w) by the total recovered volume in each tube (V_t).

$$f_o = \frac{V_o}{V_t} = 1 - f_w$$

$$f_w = \frac{V_w}{V_t} = 1 - f_o$$

3.3.2.7 Oil Recovery Factor

The oil recovery factor (RF) is calculated by dividing the difference in initial (S_{oi}) and remaining oil saturation (S_{or}) by the initial oil saturation.

$$RF = \frac{S_{oi} - S_{or}}{S_{oi}}$$

CHAPTER 4 RESULTS

This chapter compiles all the experimental results observed in this thesis. The first section characterizes the system, the second section describes the screening results with contact angles, the third section shows the spontaneous imbibition results and the last section reports the core flood results.

4.1 RESERVOIR CHARACTERIZATION

The reservoir's rock properties, brine composition, and oil properties are described in this section.

4.1.1 Rock Properties

The evaluated reservoir in this research is a high-temperature (116 °C) limestone reservoir with approximately 25% porosity and a sub-20 mD permeability. Accordingly, the initial screening tests were conducted on outcrop rock (Edwards Yellow Limestone) with similar petrophysical properties. Furthermore, both rock types had relatively similar mineralogy—Table 4.1 lists the mineralogy of both the outcrop and reservoir rocks in wt% from an X-ray diffraction test (XRD). Traces indicate values smaller than 0.5 wt%, while dashes indicate undetectable amounts. The relative petrophysical and mineralogic similarity between both rock types is the basis for ensuring representativeness and accuracy in this research. Furthermore, the tests that are conducted on outcrop rock samples significantly reduce the reservoir material requirements. While the screening experiment itself is not destructive, producing several 0.2"-thick discs would destroy valuable core plugs.

Table 4.1 – The mineralogy (wt%) of the outcrop and reservoir rocks.

Mineral Group	Mineral	Outcrop Rock	Reservoir Rock
Tectosilicates	Quartz	-	-
	Plagioclase	-	-
	Potassium Feldspar	-	-
Carbonates	Calcite	95.0	92.1
	Dolomite	1.5	5.2
	Aragonite	1.0	Traces
	Siderite	-	Traces
Phyllosilicates	Chloride	-	Traces
	Kaolinite	-	Traces
	Illite/Mica	-	1.3
Other	Pyrite	-	-
	Marcasite	-	-
	Gypsum	-	-
	Fluorite	1.3	Traces
	Anhydrite	-	-

Moreover, a mercury injection capillary pressure (MICP) test was conducted on outcrop and reservoir rock samples of 1 in. x 1 in. x 1 in. dimensions to determine the rocks' pore size distribution (Figure 4.1). The outcrop rock displayed a wide and multimodal PSD typical of carbonate rocks, spanning nearly four orders of magnitude. However, the reservoir rock showed a narrower and more normally distributed PSD. More importantly, the magnitude of the pore throat diameters (0.02-0.4 micron) is indicative of a permeability that is below 1 mD, which is contradictory with the measured

permeability. This disparity between the measured permeability and the one inferred from PSD could possibly indicate an insufficient Soxhlet extraction of the tested sample. Moreover, carbonate reservoirs are very heterogenous, whereas the tested sample has a volume of 1 in³, which is not representative of the reservoir's heterogeneity. A more accurate representation of that heterogeneity requires a significantly larger number of samples, which is not feasible due to the high materials requirement coupled with the destructive nature of the mercury injection; therefore, no attempt was made to re-test the PSD of the reservoir rock.

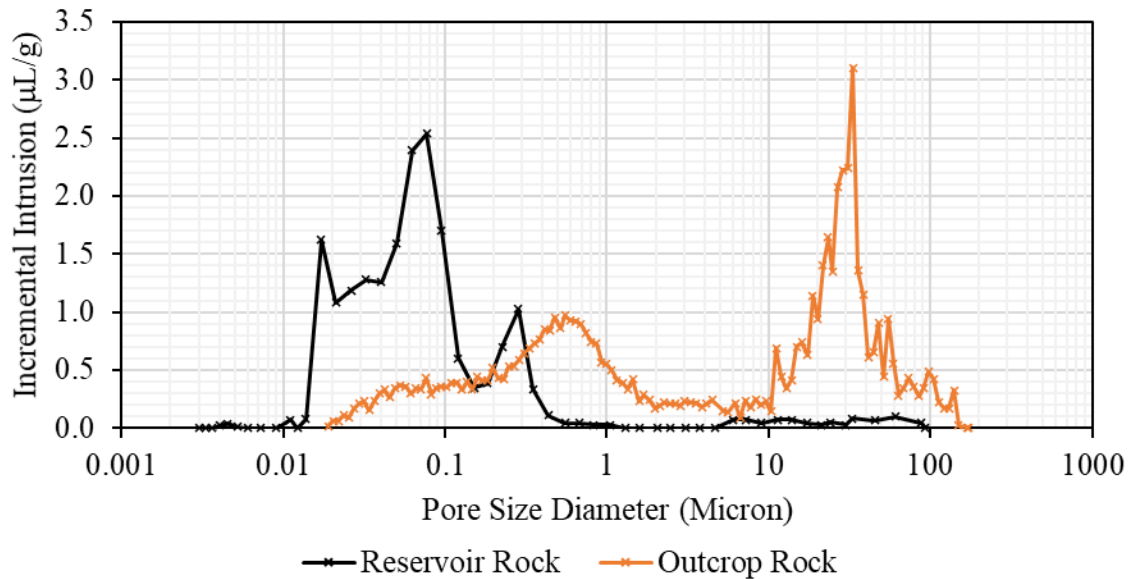


Figure 4.1 – Pore size distribution of the outcrop and reservoir rocks from MICP test.

4.1.2 Brine Composition

Injection brine (synthetic seawater) with a total salinity of 36,916 ppm was prepared by mixing reagent grade sodium chloride, magnesium chloride hexahydrate, calcium chloride dihydrate, and sodium sulfate with deionized water having a minimum resistivity of 17 MΩ-m. The brine's density and pH are 1.03 g/cm³ and 7.46,

respectively. The composition of the injection brine and formation brine are outlined in Table 4.2. While the injection brine salinity is relatively low, the hardness represents a chemical selection challenge. The formation water has a lower salinity and a significantly lower hardness; thus, the chemicals were selected and tested on the harsher of the two brines (injection brine).

Table 4.2 – The ionic composition of the injection and formation brines.

Ionic Composition	Injection Brine (ppm)	Formation Brine (ppm)
Sodium	11,667	9,608
Chloride	20,525	14,012
Carbonate	0	60
Bicarbonate	0	1,962
Calcium	401	196
Magnesium	1,372	28
Sulfate	2,951	195
Total Salinity	36,916	26,061

4.1.3 Crude Oil Properties

The reservoir oil is a light crude oil with a density of 0.83 g/cm³ (40 °API). At the reservoir temperature of 116 °C, the live oil viscosity is 0.44 cp. The dead oil viscosity at 70 °C, where the oil saturation and permeability were measured, is 2.61 cp.

Table 4.3 describes the oil's composition from SARA analysis. The oil contains approximately 10 wt% wax and less than 1 wt% asphaltene with a pour point of 30 °C. Thus, oil was heated for 24 hours at 70 °C before use or filtration to ensure consistency of the bulk and no solid dropouts or wax formation.

Table 4.3 – Crude oil composition (SARA analysis).

Component	Saturates	Aromatics	Resins	Asphaltenes
Composition (wt%)	65.4	22.1	12.3	0.2

The oil has a total acid number (TAN) of 0.11 mg-KOH/g-oil and a base number of 0.30 mg-KOH/g-oil—the acid to base ratio is 0.37. The oil’s low TAN indicates a weak tendency to result in strongly oil-wet conditions.

4.2 SURFACTANT SCREENING

4.2.1 Aqueous Stability

The aqueous stability of all 20 surfactants was tested by preparing 0.5 wt% solutions in injection brine. The tests were conducted first at room temperature to evaluate the tolerance of the surfactants to salinity and hardness, then they were tested at reservoir conditions for three days. Thirteen surfactants showed aqueous stability without any cloudiness, coagulation, or precipitation, while the remaining seven surfactants were unstable (Figure 4.2). Table 4.4 provides a summary of the unstable surfactants.

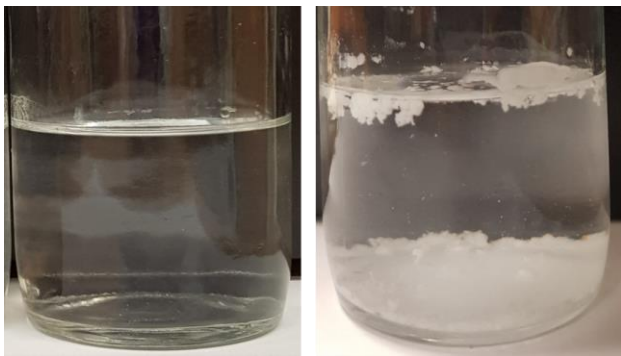


Figure 4.2 – Example of a stable surfactant (left, 0.5 wt% BTC® 8358) and unstable surfactant (right, 0.5 wt% Calimulse® PR).

Table 4.4 – Surfactants that failed the aqueous stability test.

Surfactant	Aqueous Stability
Soloterra [®] G4-12	Cloudy at reservoir temperature
Calimulse [®] PR	Precipitation at room and reservoir temperatures
Enordet [®] 0332	Cloudy at room and reservoir temperatures
Butyl Diglycol	Cloudy at reservoir temperature
2EH-2PO-50EO	Cloudy at reservoir temperature
2EH-2PO-60EO	Cloudy at reservoir temperature
Tergitol [®] NP-10	Phase separation (gel) at reservoir temperature

4.2.2 Surface Tension

The CMC of all the 13 stable surfactants was estimated by measuring the surface tension with surfactant concentration at room temperature (Table 4.5).

Table 4.5 – The CMC of aqueous stable surfactants.

Surfactant	CMC (wt%)	Surfactant	CMC (wt%)
CTAC	0.006	Calfax [®] DB-45	0.050
BTC [®] 8358	0.008	ASPIRO [®] S-2430x	0.120
Ethoquad [®] 0/12 PG	0.008	Phenol 2PO-60EO	0.002
Stepanquat [®] 3712-W	0.060	Phenol 2PO-70EO	0.004
Benzalkonium Chloride	0.010	ASPIRO [®] S-2410	0.060
Calfax [®] 16-35	0.040	Mackam [®] CB-35	0.020
Dowfax [®] 3B-2	0.060		

Figure 4.3 shows an example of the surface tensions of Phenol 2PO-70EO, Mackam[®] CB-35, and ASPIRO[®] S-2430x. From the graph, it is evident that the CMC of

ASPIRO[®] S-2430x is approximately 0.12 wt%, which is an order of magnitude higher than all the remaining surfactants. While the magnitude of the CMC is lower than the targeted 0.25 wt% concentration for testing, it is worth mentioning two important uncertainties that must be accounted for: the surfactant's activity and the effect of temperature on the CMC. Firstly, the activity of ASPIRO[®] S-2430x, for example, is 50-75%. Although the midpoint (62.5%) was used in the calculations, the difference between the mid-point and upper and lower limits is significant; an underestimation or an overestimation of the surfactant's activity can result in CMC values that are up to $\pm 20\%$ of the estimated value. Secondly, the surface tension of each surfactant was measured at room temperature; the difference between the surface tension testing conditions and the reservoir conditions is nearly 90 °C. Since the temperature difference is significant and its effect on the CMC is unknown, a safety factor was applied to the targeted surfactant concentration. Thus, the wettability-alteration screening for each surfactant was conducted at a concentration that is at least four times the surfactant's estimated CMC: 0.50 wt% for ASPIRO[®] S-2430x and 0.25 wt% for all the remaining surfactants.

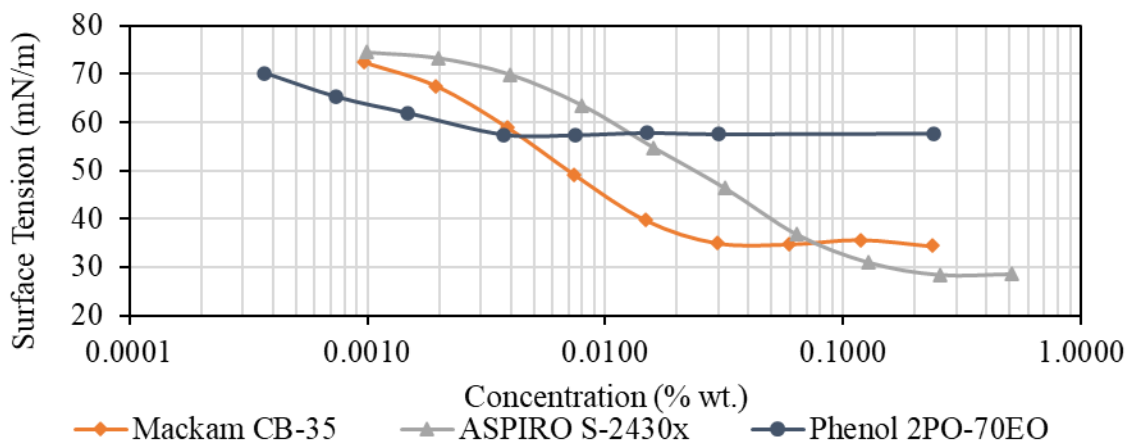


Figure 4.3 – Surface tension as a function of surfactant concentration at room temperature for three sample surfactants.

4.2.3 Wettability-Alteration Screening

One oil-wet outcrop carbonate disc was placed in a high-temperature glass cell containing brine only at reservoir conditions to establish a baseline. The shape of the oil droplets on top of the disc was monitored for 10 days (Figure 4.4). As expected, the carbonate disc did not display a strongly oil-wet behavior due to the oil's low TAN. Nevertheless, the water-advancing contact angle on this control sample was clearly higher than 130° , indicating preferentially oil-wet conditions.



Figure 4.4 – Oil-wet carbonate disc immersed in injection brine.

Similarly, 13 different oil-wet discs with the same preparation and aging conditions to the control disc were placed in each individual surfactant solution at reservoir conditions and monitored for a similar period of 10 days. The 13 discs displayed mixed results with seven discs showing signs of wettability alteration towards water-wet or intermediate-wet, while the remaining six discs did not show any significant changes in wettability (Table 4.6). Consequently, the surfactants were categorized as either wettability-altering or non-wettability-altering. The objective of the visual contact angle inspection is to provide a general, rapid screening of what surfactants alter the oil-wet carbonate disc's wettability and merit further testing; therefore, the six surfactants that did not achieve this objective were discarded.

Table 4.6 – Results of the visual wettability alteration screening.

Surfactant	Concentration (wt%)	Visual CA (°)	Wettability
CTAC	0.25	70 – 110	Altered
BTC [®] 8358	0.25	90 – 140	Altered
Ethoquad [®] 0/12 PG	0.25	120 – 150	Not Altered
Stepanquat [®] 3712-W	0.25	130 – 150	Not Altered
Benzalkonium Chloride	0.25	90 – 140	Altered
Calfax [®] 16-35	0.25	120 – 130	Not Altered
Dowfax [®] 3B-2	0.25	140 – 150	Not Altered
Calfax [®] DB-45	0.25	> 160	Not Altered
ASPIRO [®] S-2430x	0.50	70 – 100	Altered
Phenol 2PO-60EO	0.25	90 – 150	Altered
Phenol 2PO-70EO	0.25	90 – 120	Altered
ASPIRO [®] S-2410	0.25	140 – 160	Not Altered
Mackam [®] CB-35	0.25	80 – 100	Altered
Control	-	>130	-

Figure 4.5 shows two examples of the carbonate discs immersed in Ethoquad[®] 0/12 PG and ASPIRO[®] S-2430x. The difference between the two samples is stark; the sample immersed in Ethoquad[®] 0/12 PG did not show any signs of wettability alteration while the sample immersed in ASPIRO[®] S-2430x showed water-advancing contact angles that are clearly less than 90°. Pictures of all the screening samples are included in Appendix A (Figures A1-A13).



Figure 4.5 – Two carbonate discs immersed in Ethoquad® 0/12 PG (left) and ASPIRO® S-2430x (Right).

4.2.4 Contact Angle Measurements

The water-receding contact angle of the control sample and the seven candidate surfactants was measured to confirm the visual screening results. Categorically, the measured contact angles were representative of the visually observed contact angles (Table 4.7). Representative contact angles are shown in Figure 4.6.

Table 4.7 – The mean and standard deviation of the contact angle measurements for the control sample and the candidate surfactants.

Sample	Visual CA (°)	Measured CA (°)
Control (injection brine)	> 130	145 ±5
CTAC	70 – 110	51 ±7
BTC® 8358	90 – 140	110 ±11
Benzalkonium Chloride	90 – 140	104 ±20
ASPIRO® S-2430x	70 – 100	65 ±19
Phenol 2PO-60EO	90 – 150	99 ±24
Phenol 2PO-70EO	90 – 120	66 ±8
Mackam® CB-35	80 – 100	64 ±7

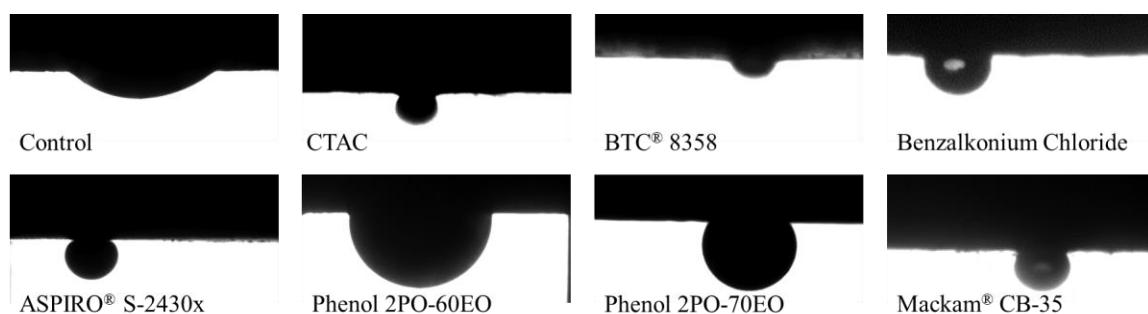


Figure 4.6 – Representative contact angle of the control sample and the surfactants that showed significant wettability alteration.

The contact angles for some of the samples showed relatively high variability, indicating a possible insufficient polishing. Nevertheless, the contact angles were categorically reproducible (Figure 4.7). The seven candidates were selected for further testing in spontaneous imbibition experiments.

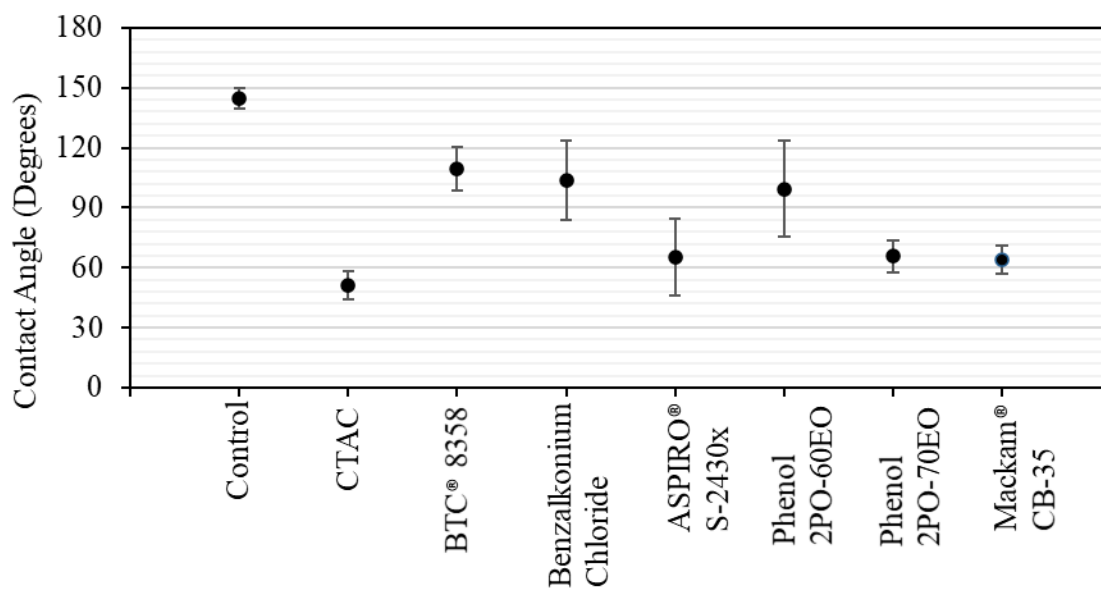


Figure 4.7 – The reproducibility of the contact angle measurements.

4.2.5 Interfacial Tension

The interfacial tension between the oil and the surfactant solutions was measured at a concentration that is consistent with the planned spontaneous imbibition and core flooding concentrations: cationic surfactants were prepared in 1.0 wt% solutions while other surfactants were prepared in 0.5 wt% solutions. Table 4.8 summarizes the IFT measurements with an average error that is less than ± 0.01 mN/m. The control sample had a low IFT that is indicative of possible contamination with surface active chemicals. Most of the surfactant solutions had a relatively similar IFT, except Phenol 2PO-60EO and Phenol 2PO-70EO, which had a relatively higher IFT as expected from the surface tension measurements and the relative size of the oil droplets during the contact angle measurements. However, this minimal variation in IFT is not expected to influence the imbibition process.

Table 4.8 – The oil/water interfacial tension of the control sample and the candidate surfactants at 100 °C.

Sample	Concentration (wt%)	IFT (mN/m)
Control (injection brine)	-	7.20
CTAC	1.0	1.40
BTC® 8358	1.0	1.15
Benzalkonium Chloride	1.0	1.47
ASPIRO® S-2430x	0.5	0.65
Phenol 2PO-60EO	0.5	3.89
Phenol 2PO-70EO	0.5	3.56
Mackam® CB-35	0.5	1.14

4.3 SPONTANEOUS IMBIBITION EXPERIMENTS

4.3.1 Outcrop Core Plugs

Two outcrop cores were dried, vacuumed, fully saturated with oil, and aged for one month. The cores were then sliced to four plugs, each. Table 4.9 shows the physical and petrophysical properties of all the eight core plugs that were used in the spontaneous imbibition experiments. The eight plugs had nearly identical lengths and diameters; thus, the impact of the aspect ratio on any gravity-driven imbibition will be similar for all the plugs. Furthermore, the porosities are relatively similar: ranging from 18.3% to 22.6%. More importantly, the permeabilities of both cores are nearly identical. Each individual plug's permeability was assumed equal to the core it was cut from. The eight plugs (1-8) were used in the following order: control, CTAC, ASPIRO[®] S-2430x, Phenol 2PO-70EO, Phenol 2PO-60EO, BTC[®] 8358, Benzalkonium Chloride, and Mackam[®] CB-35.

Table 4.9 – The physical and petrophysical properties of the spontaneous imbibition outcrop core plugs.

Plug	1	2	3	4	5	6	7	8
Length, cm	7.22	7.22	7.22	7.22	7.26	7.26	7.26	7.26
Diameter, cm	3.78	3.77	3.77	3.77	3.79	3.78	3.78	3.77
Porosity, %	22.63	21.59	19.08	21.14	19.09	21.35	19.28	18.29
Pore volume, ml	18.30	17.38	15.35	17.02	15.62	17.45	15.69	14.86
Permeability, mD	8.9				8.6			
Initial water saturation, %	0							

4.3.1.1 Oil Recovery Rate

The oil recovery rate from the core plugs was monitored for more than six months. The recovery rate was very slow due to the low permeability of the plugs (Figure 4.8). Moreover, oil recovery from the plug that was immersed in the control sample plateaued after 13 days, recovering only 4.6% of the OOIP. The low recovery factor is a good indicator of the plugs' oil-wetness and a confirmation of the appropriateness of the aging conditions. The sample immersed in Phenol 2PO-70EO was discarded after two weeks due to the experimental apparatus failure—the aqueous phase completely evaporated after approximately 10 days because of the failure of the O-ring that seals the relief valve. The remaining samples showed varying results ranging from 10.0% OOIP to 27.8% OOIP. Although oil drainage was still taking place, the experiments were stopped after 190 days to conduct other tests.

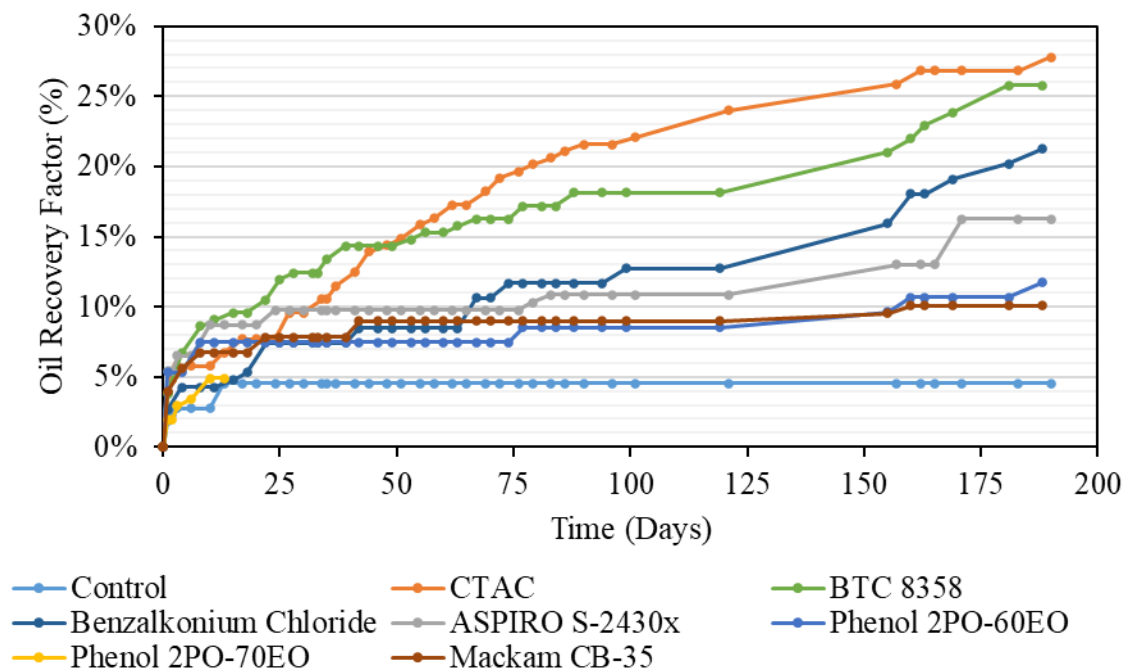


Figure 4.8 – The oil recovery rate from the oil-wet outcrop core plugs.

Figure 4.9 shows the relationship between the oil recovery factors and the contact angles. It should be noted that the oil recovery factor discussed here is not the ultimate oil recovery since most of the core plugs were still draining oil after 190 days. Generally, the oil recovery factor from the spontaneous imbibition experiment was higher at lower contact angles; however, the correlation is weak and not clear as there are two anomalies:

1. The cationic surfactants generally performed better than the non-cationic surfactants irrespective of the contact angles observed during the screening. The two samples immersed in Benzalkonium Chloride and BTC[®] 8358 recovered significantly more oil despite having contact angles of $104^\circ \pm 20^\circ$ and $110^\circ \pm 11^\circ$, respectively.

2. The non-cationic surfactants, when looked at separately, did not also correlate directly to the contact angle, as Mackam[®] CB-35 recovered considerably less oil than ASPIRO[®] S-2430x despite having nearly the same contact angle; it also recovered less oil than Phenol 2PO-60EO despite having a considerably lower contact angle and IFT.

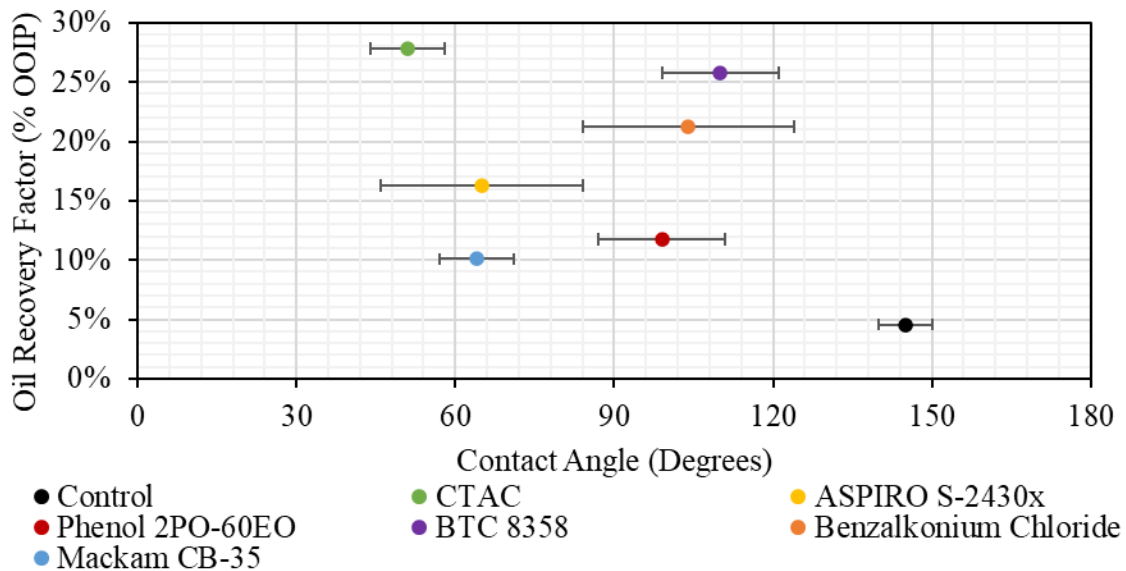


Figure 4.9 – The relationship between the contact angles and the oil recovery factors at the end of the spontaneous imbibition experiments.

Firstly, the contact angles on top of the core plug that is immersed in Benzalkonium Chloride are clearly less than 90° (Fig. 4.10), even after 24 hours only, in stark contrast to the observed contact angle during the screening experiment. Moreover, the oil drainage from the sides of the plug is indicative of counter-current water imbibition that is capillary-dominated, which would only occur if the plug's wettability was altered to preferentially water-wet. Both the carbonate plug (imbibition) and carbonate disc (screening) had similar mineralogy and aging conditions; however, there were two differences in the screening and imbibition experiments: concentration and temperature. The former was conducted at 80°C and 1.0 wt% concentration, while the latter was conducted at 116°C and 0.25 wt% concentration. While it is difficult to draw a firm conclusion from two datasets with two variables, the difference is likely due to the higher surfactant concentration, which would deem the $104^\circ \pm 20^\circ$ contact angle measured during the screening experiment as unrepresentative for the purposes of evaluating the relationship between contact angle and oil recovery factor in the imbibition experiment.

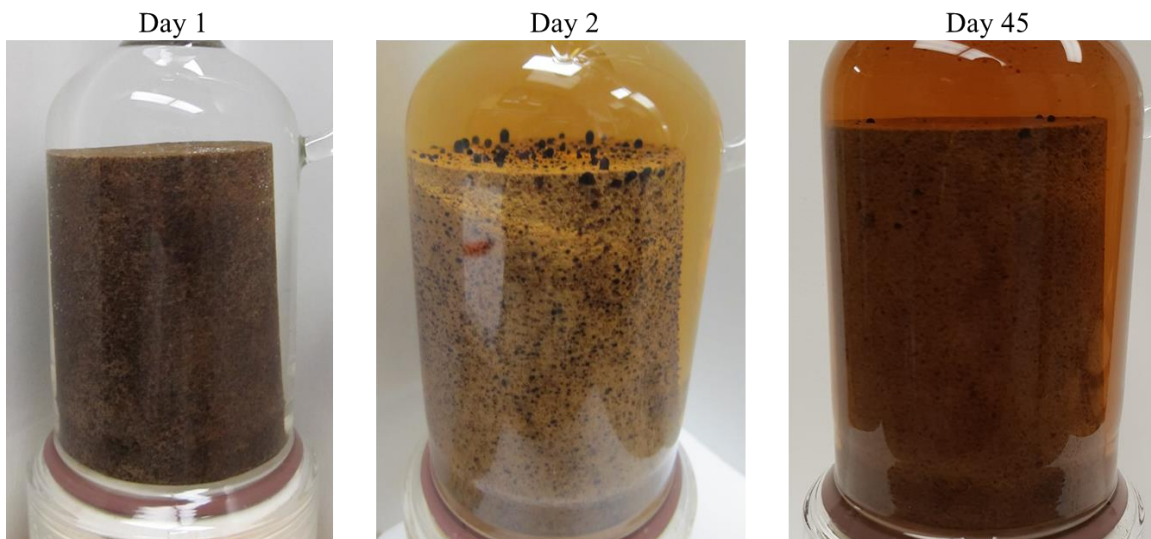


Figure 4.10 – Comparison of the core plug immersed in Benzalkonium Chloride on days 1, 2, and 45.

Secondly, the sample immersed in BTC[®] 8358 showed a unique behavior. Unlike Benzalkonium Chloride and CTAC, all the initial oil drainage occurred from the top surface of the plug only, without any oil drainage from the sides of the plug (Figure 4.11). Furthermore, the shape of the oil droplets on top of the plugs are noticeably different: BTC[®] 8358 was clearly displaying oil-wet behavior on the second day of evaluation contrasting with the other two cationic surfactants. From this, it can be inferred that unlike Benzalkonium Chloride, the increase in concentration from 0.25 wt% to 1.0 wt% is likely not responsible for this high oil recovery factor from BTC[®] 8358 since the contact angle observed during the imbibition experiment was not any better than the contact angle observed during the screening experiment. The IFT of this sample (1.15 mN/m) is relatively lower than most samples, but the difference is very minimal and highly unlikely to be the reason behind this higher recovery factor.

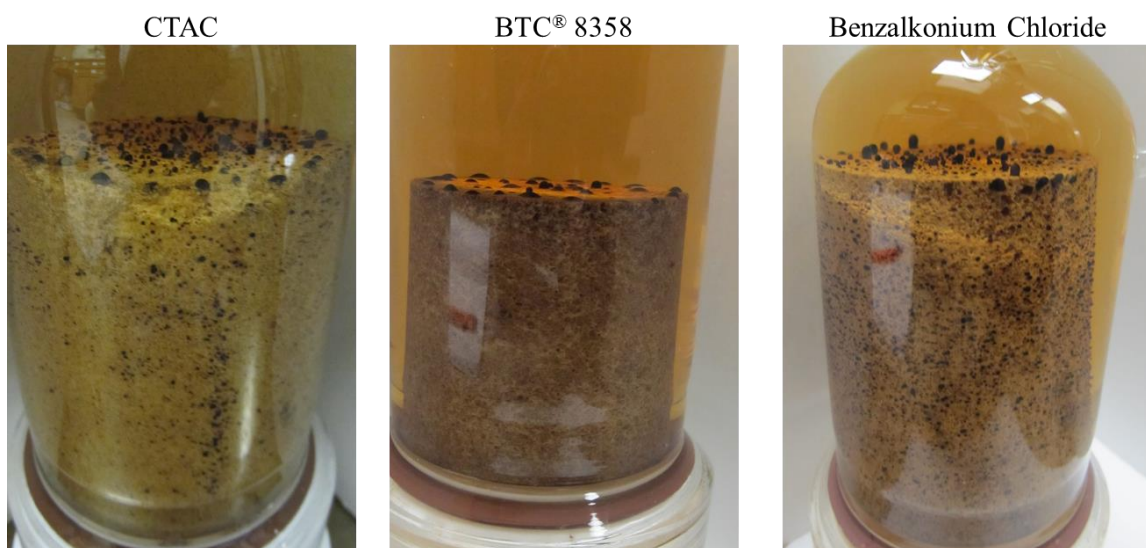


Figure 4.11 – Comparison between the core plugs immersed in CTAC, BTC[®] 8358, and Benzalkonium Chloride on day 2.

A closer look at the plug's top surface at different time intervals reveals an interesting behavior: the contact angle is lower with time, albeit slight (Figures 4.12 &

4.13); on day 45 the surface appears mixed-wet rather than oil-wet. However, most of the oil drainage from this sample occurred during the first month of the experiment, where 14.3% OOIP was recovered during the first 40 days. Therefore, the change in wettability at later times does not explain this relatively rapid early-time recovery rate. One possible explanation is that the permeability of this plug was underestimated. A comparison of the four plugs that were cut from the second core shows that the plug immersed in BTC[®] 8358 has a porosity that is 2-3% higher than the other three plugs. The porosity difference supports but does not confirm this explanation.

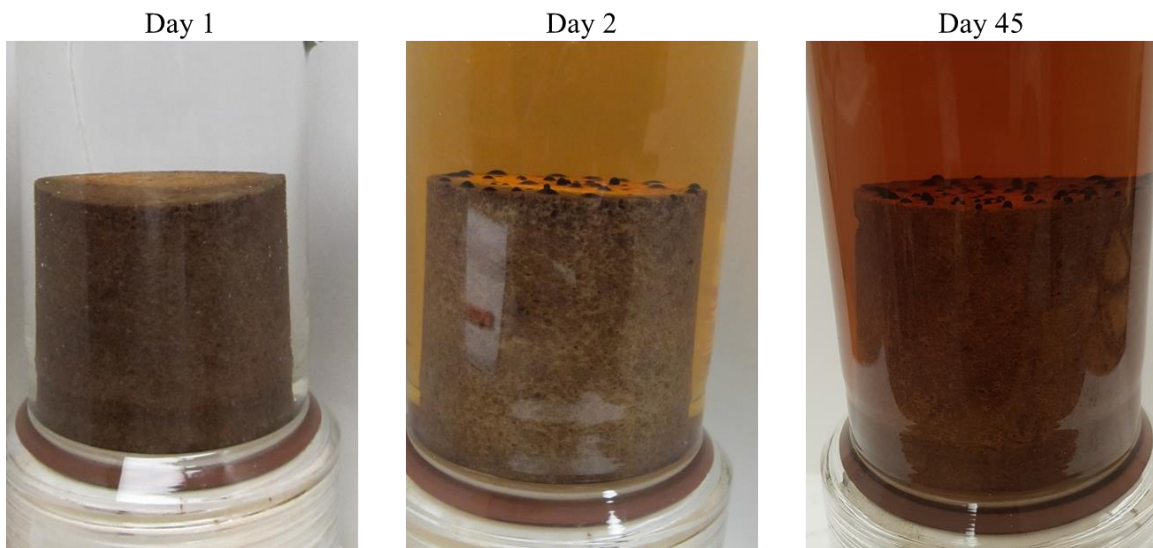


Figure 4.12 – Comparison of the plug immersed in BTC[®] 8358 at days 1, 2, and 45.



Figure 4.13 – Comparison of the top surface of the core plug immersed in BTC[®] 8358 at days 2 and 45.

Unfortunately, beyond the second month, the aqueous phase became very dark and it was nearly impossible to detect any oil droplets at later times to confirm the change in contact angle with respect to time; in fact, this was the darkest evaluated sample. Figure 4.14 shows an example where the color of the aqueous phase of four different samples is compared. The darker aqueous phase indicates a high degree of oil solubilization, which could offer another explanation to the higher oil recovery factor from this sample.

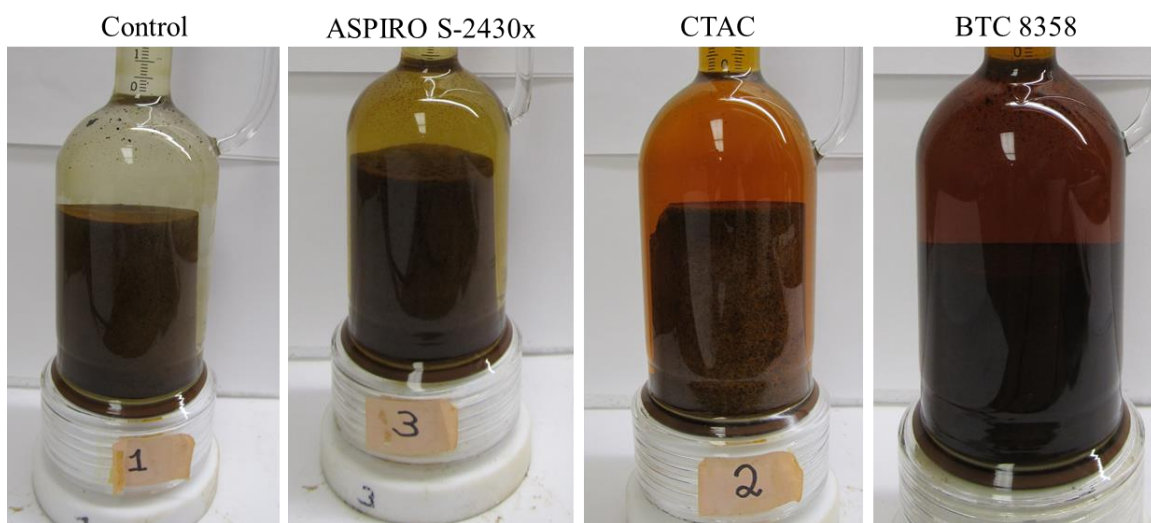


Figure 4.14 – Comparison of the aqueous phase of four samples on the last day of spontaneous imbibition.

Lastly, the sample immersed in Mackam[®] CB-35 merits a special consideration. This is the only zwitterionic surfactant used in this research. More importantly, among the seven surfactants used in the spontaneous imbibition experiments, it is the only surfactant containing a negative charge in the hydrophilic head group. The contact angle on top of the core plug was categorically consistent with the observed contact angle in the screening experiments (Figure 4.15). Yet, the recovery was significantly lower than ASPIRO[®] S-2430x, which has a relatively similar contact angle. It was also slightly

lower than Phenol 2PO-60EO, which has a significantly higher contact angle and IFT. It is highly likely that the low recovery factor despite the low contact angle and IFT is due to the surfactant consumption (adsorption). Looking closely at the recovery rate graph, oil drainage from the sample immersed in Mackam[®] CB-35 ceased after 42 days; this is the only sample where imbibition was not taking place at the time of termination. The minimal increase between days 155-160 is caused by handling, as it is merely resulting from the release of the oil droplets adhering to the plug's top surface.

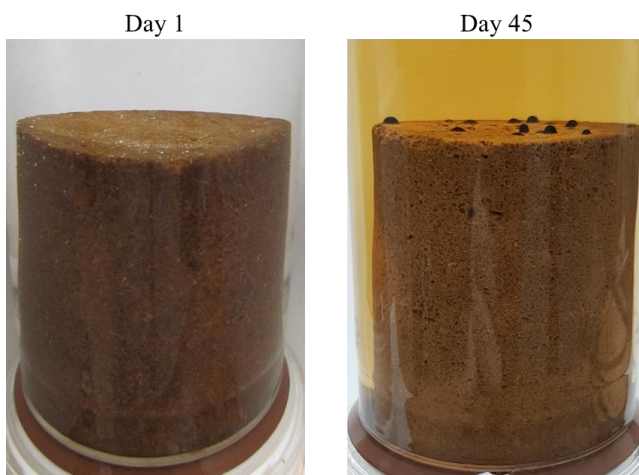


Figure 4.15 – Comparison of the core plug immersed in Mackam[®] CB-35 at days 1, and 45.

4.3.1.2 Plug Cleaving

All seven core plugs were axially cleaved through the center to gain a better insight on the shape of the waterfront, with the aim of establishing a water imbibition mechanism that explains the discrepancy in the imbibition results. Unfortunately, the waterfront on some core plugs was undiscernible, even under an ultraviolet light source. Therefore, the images were digitally contrasted to sharpen the shape of the front, which greatly helped in defining the areas contacted by water without affecting the integrity of the images. In all the images in this section, the lighter color represents the aqueous

phase, whereas the darker color represents the oleic phase. Furthermore, the images are provided in both raw and contrasted formats.

It is interesting that both nonionic surfactants (ASPIRO[®] S-2430x and Phenol 2PO-60EO) showed water accumulation at the bottom of the cleaved core plugs, indicating a gravity-driven water imbibition (Figures 4.16 and 4.17). The result is expected in the case of Phenol 2PO-60EO since its contact angle was relatively high (99°). However, in the case of ASPIRO[®] S-2430x, it indicates that the effect of IFT is greater than the effect of the contact angle, despite the oil recovery correlating to both factors (Figures 4.18 and 4.19).



Figure 4.16 – The cleaved core plug immersed in ASPIRO[®] S-2430x.

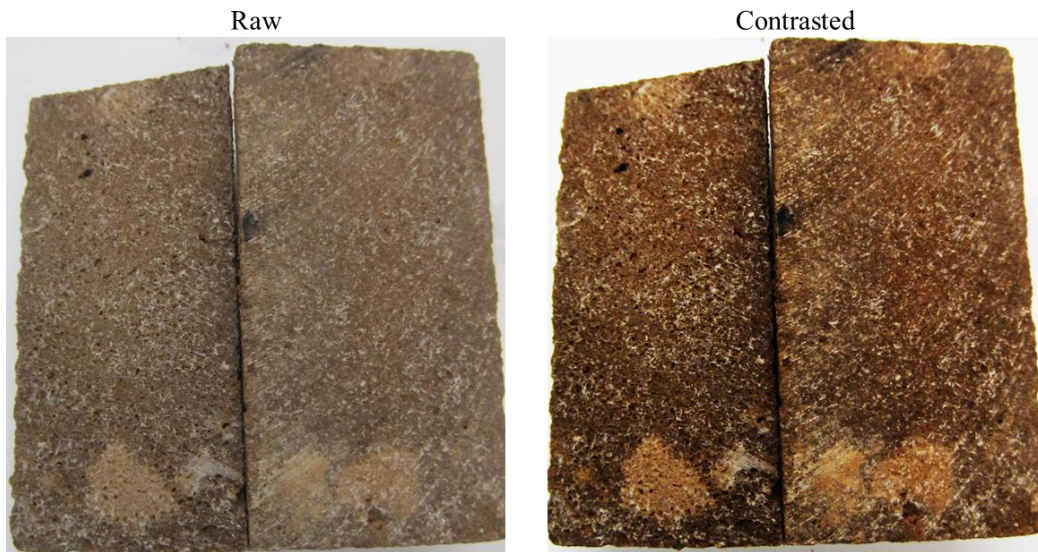


Figure 4.17 – The cleaved core plug immersed in Phenol 2PO-60EO.

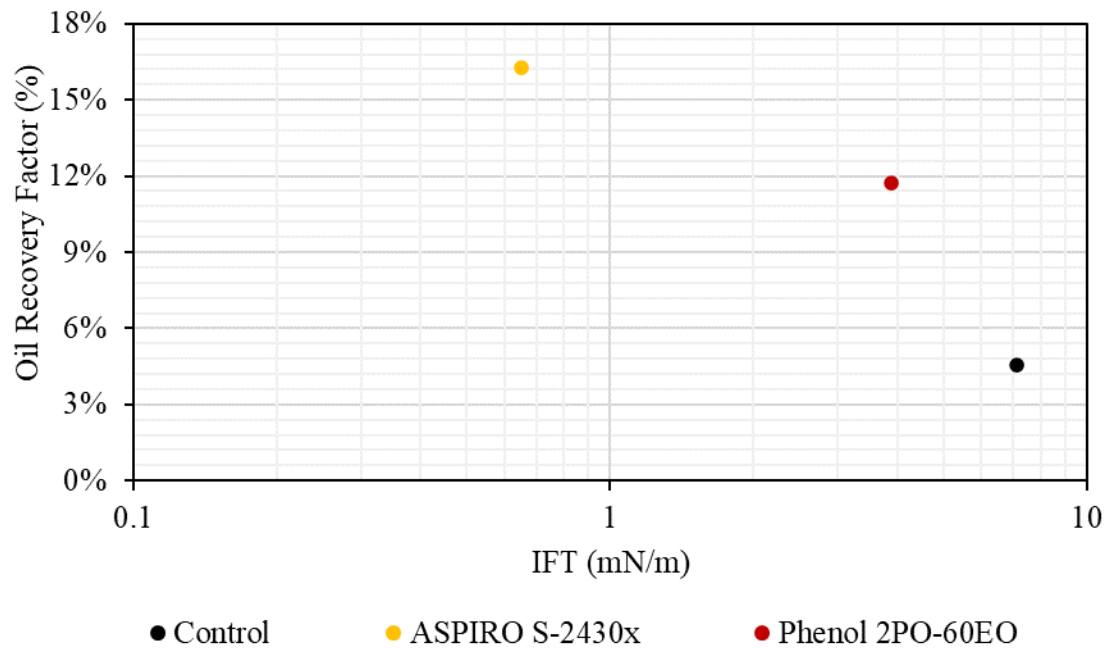


Figure 4.18 – The relationship between the oil recovery factor and the IFT of the nonionic surfactants.

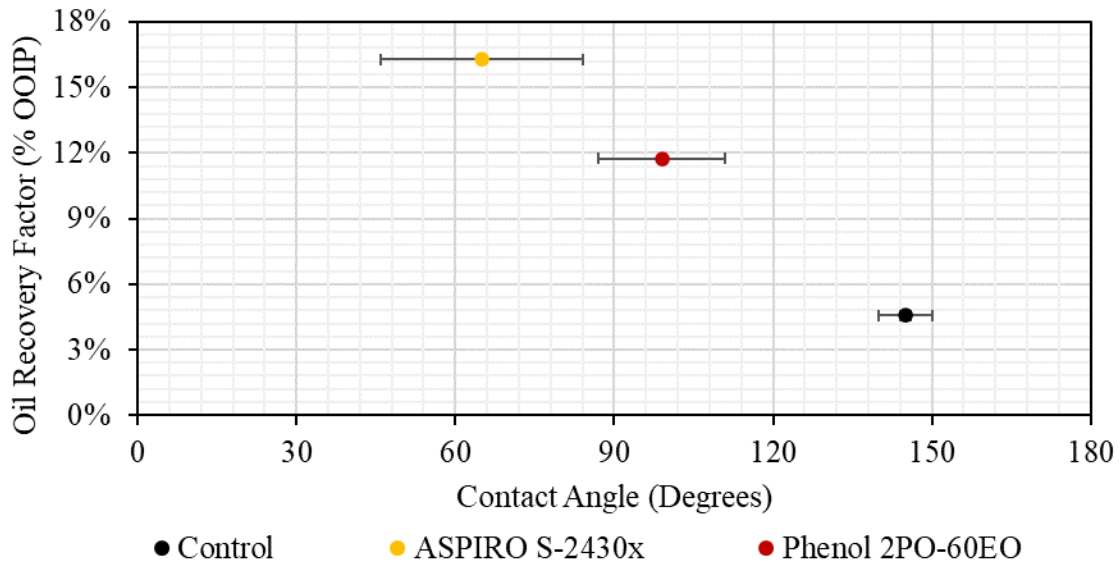


Figure 4.19 – The relationship between the oil recovery factor and the contact angle of the nonionic surfactants.

Moreover, the cleaved core plug immersed in the cationic surfactant BTC[®] 8358 shows a completely different imbibition mechanism, whereby water is clearly imbibing the plug from all directions (Figure 4.20). The shape of the waterfront indicates a capillary-driven water imbibition; therefore, its higher-than-expected recovery cannot be solely attributed to its marginally lower IFT. It is interesting to note how deep the waterfront is since the oil recovery factor of around 26% OOIP does not suggest such a deep water invasion.

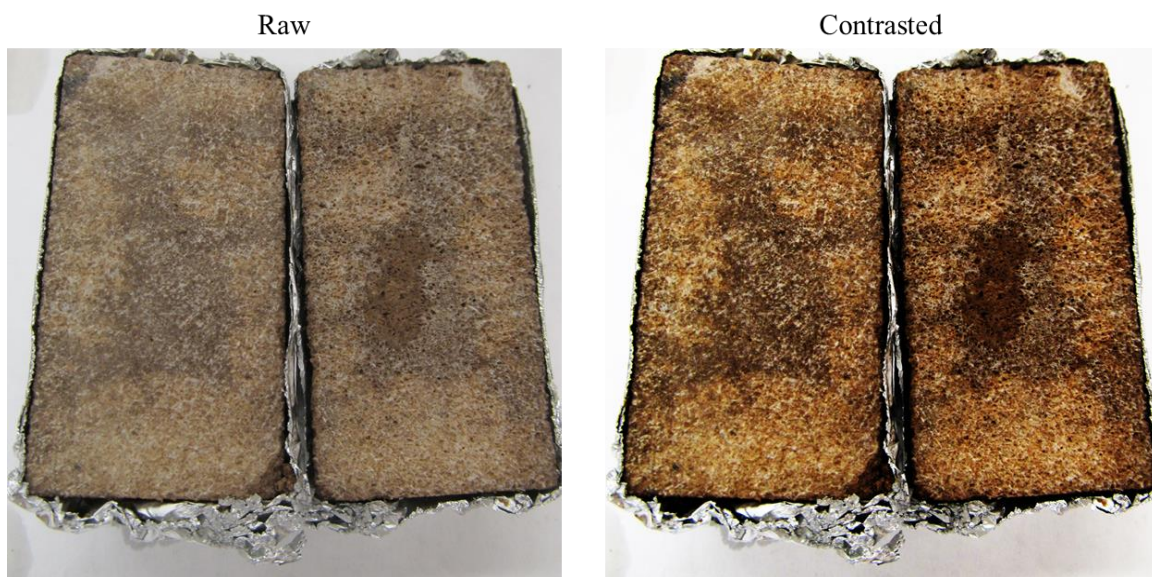


Figure 4.20 – The cleaved core plug immersed in BTC[®] 8358.

Lastly, the core plug immersed in Mackam[®] CB-35 displayed a relatively similar waterfront to the one observed in BTC[®] 8358, albeit to a lesser extent (Figure 4.21). One half (right) of the cleaved plug was visibly damaged by the saw blades during the cleaving process, but the other half (left) clearly shows water imbibing from the sides of the plug. The waterfront is not deep due to the low recovery factor of 10% OOIP from this sample. Nevertheless, this capillary-driven water imbibition further supports that the low recovery factor from this core plug is not ensuing from the inaccurate measurement of the contact angle, but rather possibly due to the loss of surfactant as a result of adsorption.

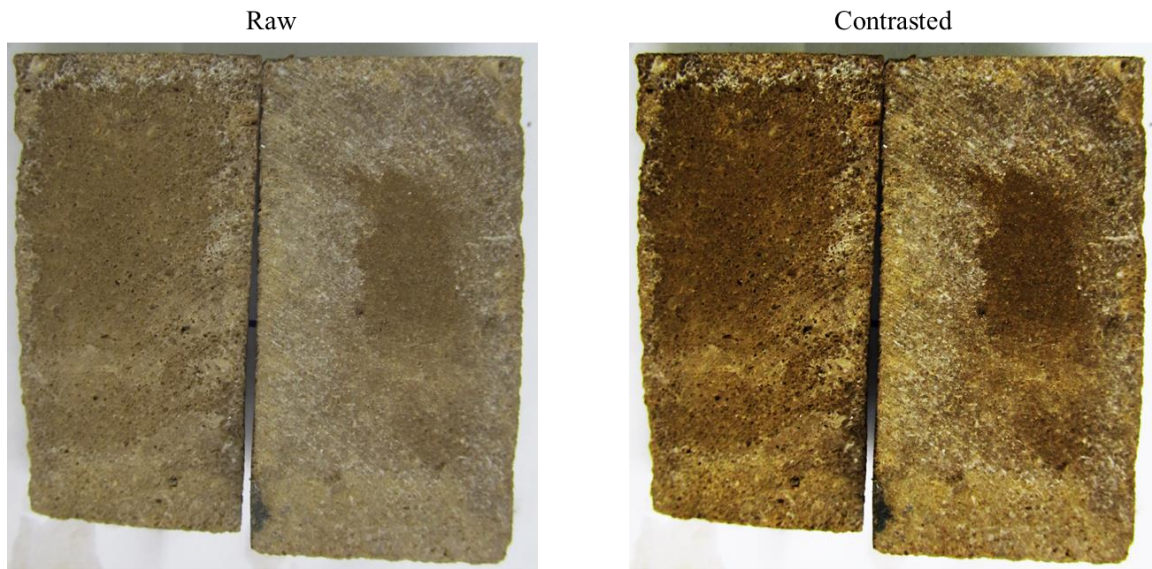


Figure 4.21 – The cleaved core plug immersed in Mackam[®] CB-35.

4.3.2 Reservoir Core Plugs

To evaluate the representativeness of the outcrop imbibition experiment and its applicability to the reservoir under evaluation, the spontaneous imbibition experiment was repeated on three reservoir core plugs. A composite reservoir core was cleaned, dried, vacuumed, fully saturated with oil, and aged for 1 month. Table 4.10 shows the physical and petrophysical properties of the three core plugs. The plugs were immersed in a control sample in addition to the top two performing surfactants in the outcrop imbibition experiments: CTAC and BTC[®] 8358. The surfactants were used at a similar and consistent concentration of 1.0 wt%.

Table 4.10 – The physical and petrophysical properties of the spontaneous imbibition reservoir core plugs.

Plug	1	2	3
Length, cm	6.47	8.41	7.40
Diameter, cm	3.77	3.77	3.78
Porosity, %	24.50	22.27	26.83
Pore volume, ml	17.66	20.85	22.25
Permeability, mD	5.4		
Initial water saturation, %	0		

4.3.2.1 Oil Recovery Rate

The oil recovery rate from all three samples was monitored for four months and is currently still ongoing. After 120 days, the oil recovery of the control sample was 6.3% OOIP, while the two surfactants BTC® 8358 and CTAC have fared significantly better, recovering 13.9% and 15.2% OOIP, respectively (Figure 4.22).

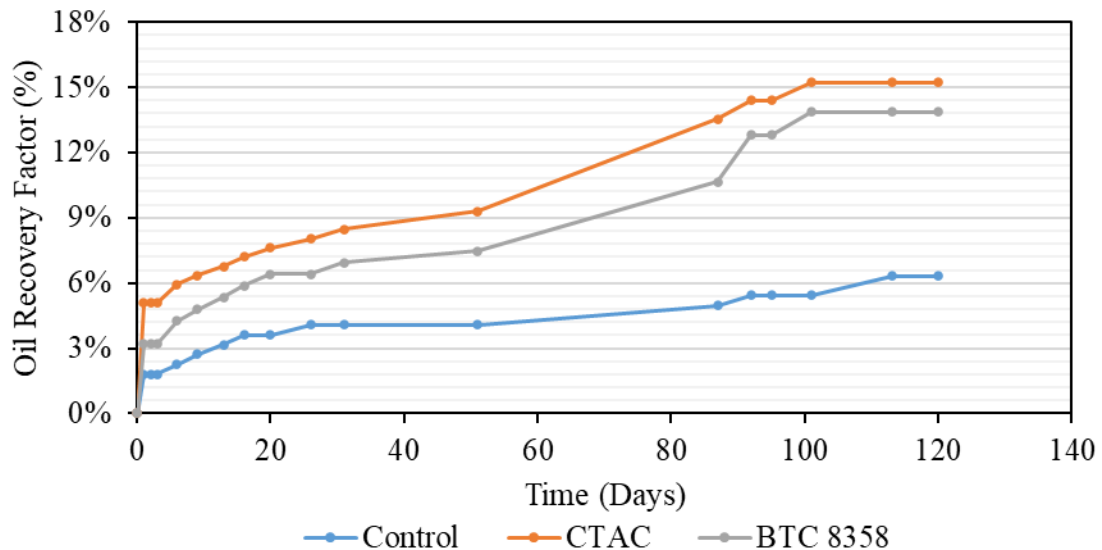


Figure 4.22 – The oil recovery rate from the oil-wet reservoir core plugs.

Figure 4.23 compares the recovery rates from the outcrop core plugs and the reservoir core plugs. The recovery rate of the reservoir control sample was relatively similar to the outcrop control sample with an oil recovery factor of 6.3% OOIP. Moreover, the reservoir control sample was still imbibing water after at least 113 days as opposed to the outcrop control sample, which plateaued at day 13. It should be noted, however, that the reservoir core plugs had lower permeability than the outcrop core plugs. Even though the reservoir control sample continued to imbibe water for a longer period, a similar 4.6% OOIP recovery was not attained until two months of imbibition have elapsed. The difference in recovery rates between the outcrop and reservoir plugs immersed in both surfactants was more pronounced: the samples immersed in CTAC were nearly identical for the first 26 days and diverged afterwards, while the samples immersed in BTC® 8358 were incomparable.

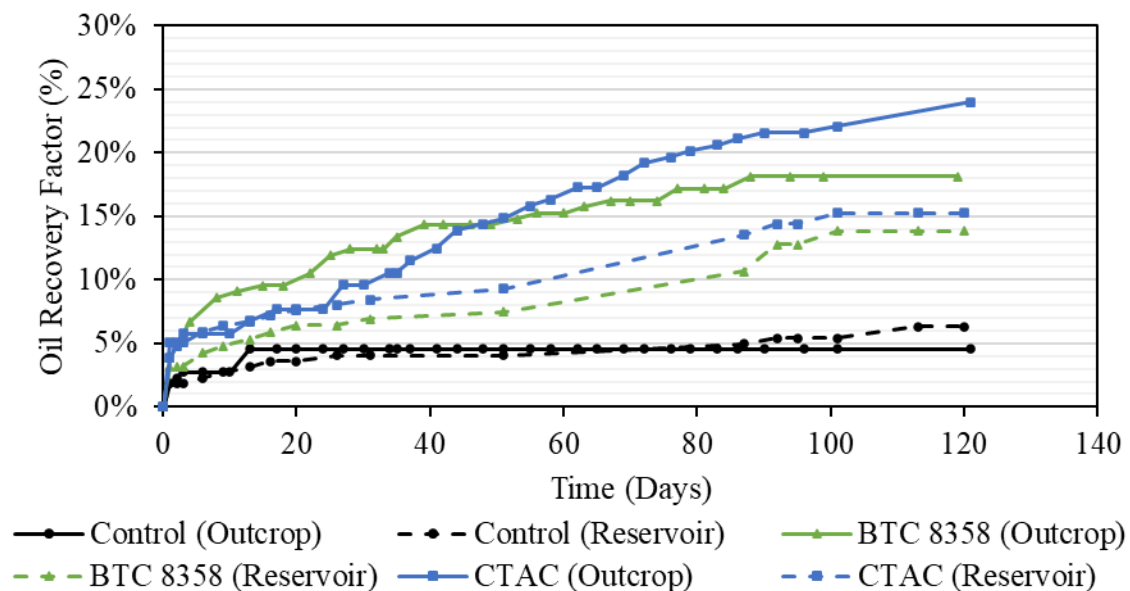


Figure 4.23 – Comparison between the recovery rates from the outcrop core plugs (solid) and the reservoir core plugs (dashed).

The comparison between the recovery rate among the two series is somewhat inaccurate as the physical (aspect ratio) and petrophysical (porosity and permeability) properties of both sets of plugs is different. An attempt to scale the data using the equations described in section 3.3.1.3 reveals a better representation of the spontaneous imbibition results. The scaling takes the plug's length, diameter, permeability, and porosity into consideration, thus yielding a better basis for comparison. (Figure 4.24). However, it is important to mention that a major assumption was made in assuming that each plug's permeability was similar to the permeability of the core it was cut from. The nondimensional time in the scaling (t_D) is a function of the square root of permeability; thus, minor variations in permeability are not expected to have a pronounced effect on the curves, but large permeability underestimations or overestimations will significantly affect the curves. Therefore, it is important to treat the scaling results qualitatively rather than quantitatively

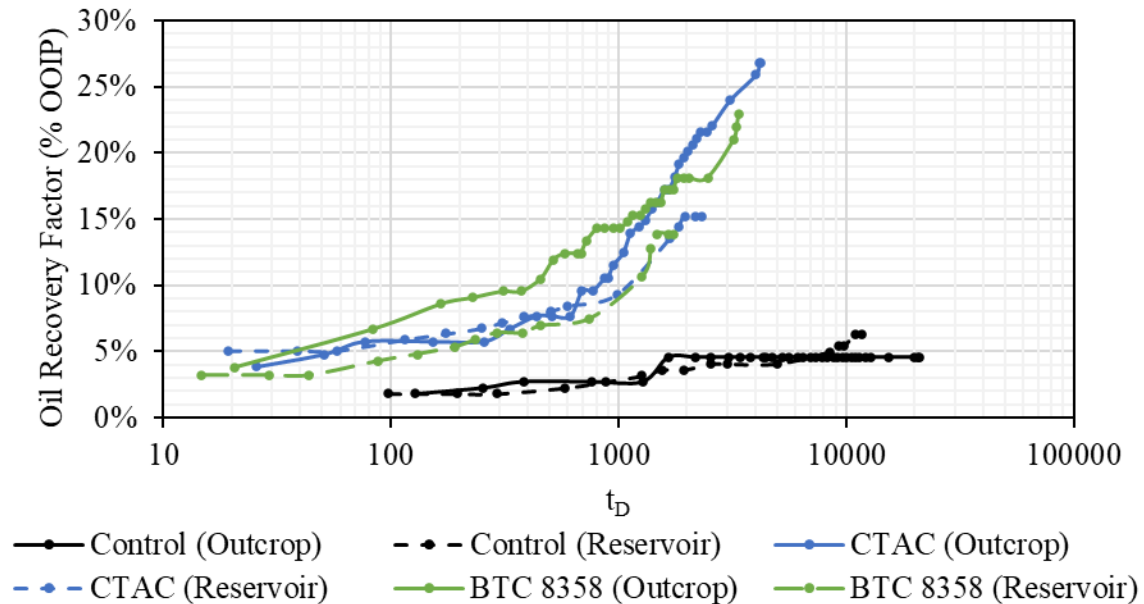


Figure 4.24 – Comparison between the recovery rate from the outcrop plugs (solid) and the reservoir plugs (dashed) using non-dimensional time (t_D).

After scaling the oil recovery data using the nondimensional time, the similarity between the outcrop and reservoir experiments became clearer. The curves of the control sample and CTAC are relatively similar. However, the plugs immersed in BTC[®] 8358 were markedly different, especially during early to intermediate times, where both curves were clearly divergent. However, at later times, the results of the two experiments started to converge. This corroborates with the uncertainty surrounding the high early-time recovery rate of BTC[®] 8358 during the outcrop experiment, and further raises questions about the possible underestimation of the outcrop plug's permeability.

4.4 CORE FLOODS

The core flood experiment is described in this section.

4.4.1 Core Description

One core flood experiment was conducted with the objective of testing the efficacy of wettability alteration in enhancing oil recovery from a 1-ft.-long core. CTAC was selected based on its promising contact angle and spontaneous imbibition performance. The surfactant was prepared in 1.0 wt% solution that is consistent with the spontaneous imbibition experiment. Table 4.11 shows the physical and petrophysical properties of the used core. The core was oven-dried, vacuumed, fully saturated with filtered crude oil, and aged for 28 days. Prior to the core flooding experiment, the oil inside the core was refreshed by injecting 2 PV of crude oil.

Table 4.11 – The physical and petrophysical properties of the core flooding core.

Core Flood #	1
Core Type	Edwards Yellow
Length (cm)	29.37
Diameter (cm)	3.80
Porosity (%)	25.28
Pore Volume (cm ³)	84.13
Permeability (md)	19.8
Initial S _o (%)	100

4.4.2 Core Flood 1

Two pore volumes (PV) of synthetic seawater were injected at a rate of 0.03 ml/min ($v = 0.5$ ft./day). After injecting two PVs of water, 64.2% of the oil was recovered. Despite the core's aging for nearly one month, the high recovery factor from the waterflood coupled with the sharp decline in oil cut and high waterflood efficiency do not imply strongly oil-wet conditions, which was expected from the contact angle measurements and the oil's low TAN (Figure 4.25). Following the injection of 2PV seawater, a slug of 1 wt% CTAC equivalent to the volume of water in the core (0.64 PV) was injected. The surfactant flood was then shut-in to for soaking. Although the plan was to shut-in the injection for around 7-10 days, the shut-in time was extended to 77 days due to extenuating circumstances. After soaking, the injection of surfactant into the core was resumed at a similar injection rate. After injecting an additional 1.1 PV, a sizeable oil bank broke through, with an incremental oil gain (ΔS_o) of 19.6%, nearly half the remaining oil in the core.

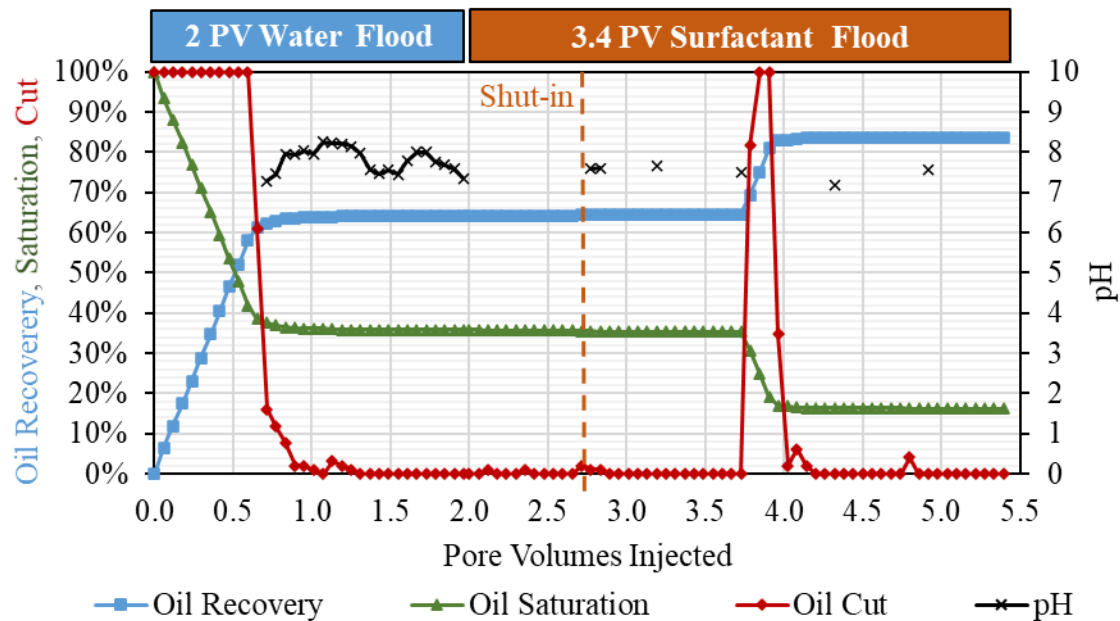


Figure 4.25 – Core flood 1 effluent analysis.

Figure 4.26 shows the pressure drop across the core during the core flood. The high noise in the pressure data during the waterflood (0-2 PV) is likely a result of trapped gas bubbles in the pressure transducer lines; both the inlet and the outlet lines were purged with deionized water after the waterflood to eliminate any trapped gas. The steady-state pressure drop at the residual oil saturation after waterflood (S_{orw}) is approximately 2.1 psi, indicating an end-point water relative permeability (k_{rw}^o) of 0.11, which does not imply strongly oil-wet state. The pressure drop remained relatively constant at around 2.1 psi after injecting the initial surfactant slug. Similarly, the soaking period did not have a material impact on the pressure drop initially. At around 3.25 PVI (0.56 PV after the shut-in), the pressure drop increased rapidly to around 7.5 psi, where the oil bank broke through. The pressure drop then stabilized at approximately 6.3 psi, implying a reduction in the end-point water relative permeability from 0.11 to 0.04 although the water saturation increased significantly from 64.2% to 83.8%. This high

increase in pressure at a higher water saturation is likely a result of the oil's drainage from the smallest pores, followed by mobilization and then entrapment in the larger pores. The oil's entrapment at the largest pores forces the water to flow through the narrower pores, thus resulting in a higher pressure drop, and consequently lower relative permeability.

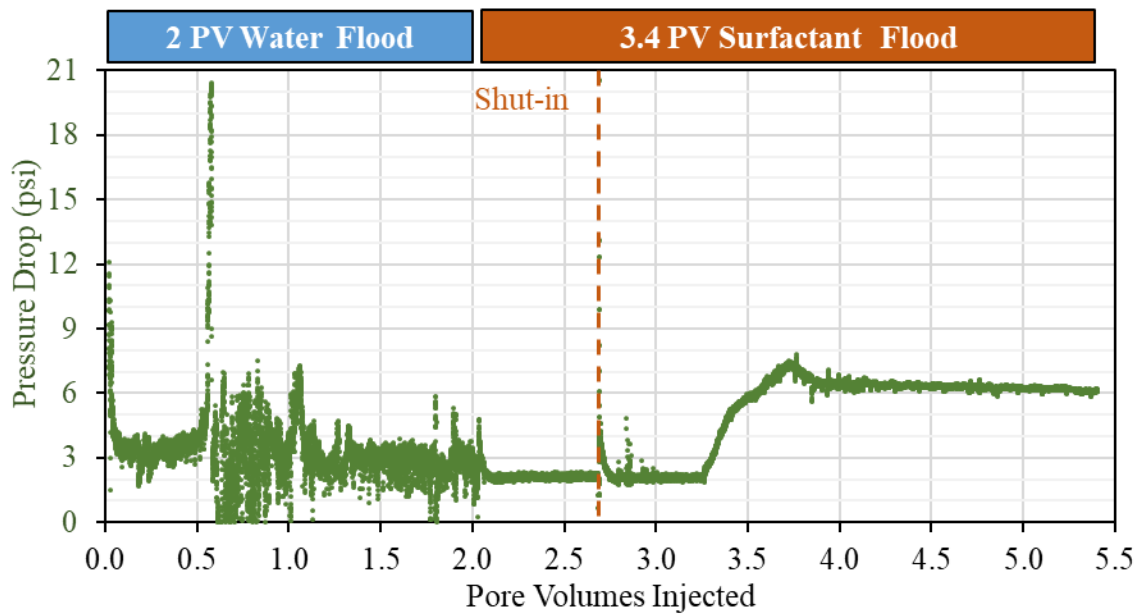


Figure 4.26 – Core flood 1 pressure drop.

CHAPTER 5 CONCLUSIONS

This chapter summarizes the conclusions drawn from the experimental investigation of this research and provides recommendations for future work.

5.1 SYSTEMATIC SCREENING & TESTING

This research provided a systematic framework to screen and test various surfactants for their efficacy at enhancing oil recovery from a high-temperature, high-hardness, tight carbonate reservoir via wettability alteration. The basis of screening lies in identifying an appropriate outcrop rock for initial testing, which is based on its similarity to the reservoir rock's mineralogy and petrophysical properties. The proper outcrop selection reduced the reservoir material requirements and provided representative and cost-effective initial results.

Thereafter, polished outcrop carbonate discs of 0.2 in. (L) \times 1.5 in. (D) dimensions were aged in oil and then immersed in different surfactant solutions to evaluate each surfactant's effectiveness at altering the discs wettability. The wettability alteration was quantified by measuring the contact angle an oil droplet forms on each disc. The selection of actual carbonate discs in lieu of the oft-used calcite chips provide more representative results if carefully handled and polished to reduce the effects of surface roughness.

By virtue of elimination, the most effective surfactants at reducing the contact angles are then tested on 3 in. (L) \times 1.5 in. (D) core plugs to evaluate changes in the oil recovery rate from spontaneous imbibition experiments due to wettability alteration. Lastly, the top performing surfactants are then tested on 1 ft. long core with 1.5 in. diameter, where the core is waterflooded to residual oil saturation, then flooded with a

surfactant to assess changes in the residual oil saturation. The spontaneous imbibition experiment was then replicated on reservoir rock samples using the most effective surfactants, thereby optimizing the material requirements.

5.2 WETTABILITY ALTERATION

The systematic selection, testing, and screening of 20 surfactants of varying classes, chain lengths, and functional groups yielded seven surfactants that significantly reduced the measured contact angles, thereby successfully altering the evaluated carbonate's wettability towards intermediate-wet (Phenol 2PO-60EO, Benzalkonium Chloride, and BTC[®] 8358) or preferentially water-wet (CTAC, ASPIRO[®] S-2430x, Mackam[®] CB-35, and Phenol 2PO-70EO). The wettability-altering surfactants were cationic (3), nonionic (3), or zwitterionic (1), whereas none of the six tested anionic surfactants have shown a potential for wettability alteration.

The spontaneous imbibition experiments conducted for more than six months on the wettability-altering surfactants resulted in oil recoveries that are two to six times the oil recovery of the control sample containing no surfactant (4.6% OOIP). Out of the six tested surfactants, the three cationic surfactants (CTAC, BTC[®] 8358, and Benzalkonium Chloride) had significantly higher recoveries ranging from 21.2% to 27.8% OOIP, compared to the non-cationic surfactants' recoveries that ranged from 10.0% to 16.3% OOIP. Among which, the sample immersed in the zwitterionic surfactant Mackam[®] CB-35 stopped imbibing water after 42 days, probably due to adsorption. Axial cuts of the two core plugs immersed in the two nonionic surfactants ASPIRO[®] S-2430x and Phenol 2PO-60EO indicated a gravity-dominated imbibition.

The spontaneous imbibition experiments were replicated on three reservoir core plugs, using a control sample and the top two performing surfactants in the outcrop

experiments (CTAC and BTC[®] 8358). Both surfactants performed comparatively well after 4 months, recovering 15.2% OOIP and 13.9% OOIP, respectively, as opposed to the control sample's recovery of 6.3% OOIP. Scaling of the recovery rates using the equations from Ma et al. (1997) described in section 3.3.1.3 showed relative similarity between both rock types, proving the appropriateness of the outcrop selection.

5.3 ENHANCED OIL RECOVERY

The results of the spontaneous imbibition experiments prove the changes in wettability but do not necessarily imply changes in residual oil saturation. Due to the destructive nature of the plug's cleaving, the plugs were not suitable for forced imbibition experiments to evaluate changes in residual oil saturation. Rather, the effectiveness of wettability alteration at enhancing oil recovery was tested through a core flooding experiment on a 1 ft. (L) \times 1.5 in. (D) core.

The core flooding experiment was conducted with the top performing surfactant CTAC, which had a contact angle of $51^\circ \pm 7^\circ$ and oil recovery of 27.8% in the spontaneous imbibition experiment. The outcrop core was fully saturated with crude oil and aged for one month, then waterflooded to a residual oil saturation (S_{orw}) of 35.8%, before being flooded with 1.0 wt% CTAC. After 0.64 PV of surfactant solution injection, the flood was stopped for 77 days soaking time, and then the flow was resumed. The use of CTAC resulted in significant incremental oil recovery (ΔS_o) of 19.6%, substantially reducing the residual oil saturation from 35.8% to 16.2%. The results of the core flooding experiment prove that CTAC not only altered the core's wettability, but also consequently reduced the core's residual oil saturation significantly. It also shows that wettability alteration is a sound strategy to enhance oil recovery from tight, high-temperature, and high-hardness carbonate reservoirs.

5.4 FUTURE WORK RECOMMENDATIONS

This research provided a framework to screen and test surfactants for their potential in altering the wettability of a tight, high-temperature, high-hardness carbonate reservoir. Furthermore, it demonstrated the efficacy of CTAC in significantly enhancing oil recovery via wettability alteration. Nonetheless, there are a few prospective studies that merit further investigation from both a technical and economic considerations.

The surfactant concentrations used in this research are relatively high (0.5-1.0 wt%). A sensitivity analysis on the efficacy of wettability alteration as a function of surfactant concentration is necessary to optimize the material requirements. As shown by the samples immersed in Benzalkonium Chloride, the degree of wettability alteration was significantly different for the two samples immersed in 1.0 wt% and 0.25 wt% solutions although both concentrations were significantly higher than the surfactant's CMC of 0.01 wt%.

In addition, the soaking shut-in period during the core flood was originally designed to last for 3-7 days. Due to extenuating circumstances, the shut-in period was extended to 77 days, which is excessively unrealistic in a lab setting (not excessive for field setting). The wettability screening on the carbonate discs indicate that the surfactants have generally achieved their wettability alteration objective after 3-7 days. A sensitivity analysis of the shut-in soaking time is necessary to reduce the time-requirement of the experiment.

Additionally, the amount of surfactant used in the tertiary recovery stage (4 PV) is high and possibly uneconomical. The wettability alteration is expected to be achieved by the first surfactant slug that was injected after the waterflood. Therefore, a more economically plausible alternative is to replace the surfactant flood post the soaking shut-

in period with brine and evaluate whether this achieves the same objective as this would reduce the required amount of surfactant by approximately 80%.

Moreover, no effort was made to measure the surfactant retention during the core flood. Due to the cationic nature of the surfactant, its adsorption on the carbonate rock's surface is not expected to be high. Therefore, analysis of the surfactant retention coupled with the concentration requirement would result in a lower surfactant concentration that might achieve the same objective at a fraction of the cost.

Lastly, the results of the spontaneous imbibition experiment were categorically reproducible between both the outcrop and the reservoir rocks; however, the core flood experiment needs to be replicated on a reservoir core to evaluate whether the core flooding results are also reproducible between both sets of rocks.

APPENDIX A – SCREENING PICTURES



Figure A1 – ASPIRO® S-2430x initial screening.



Figure A2 – Calfax® 16-35 initial screening.



Figure A3 – ASPIRO® S-2410 initial screening.



Figure A4 – CTAC initial screening.



Figure A5 – BTC[®] 8358 initial screening.



Figure A6 – Dowfax[®] 3B-2 initial screening.



Figure A7 – Calfax® DB-45 initial screening.

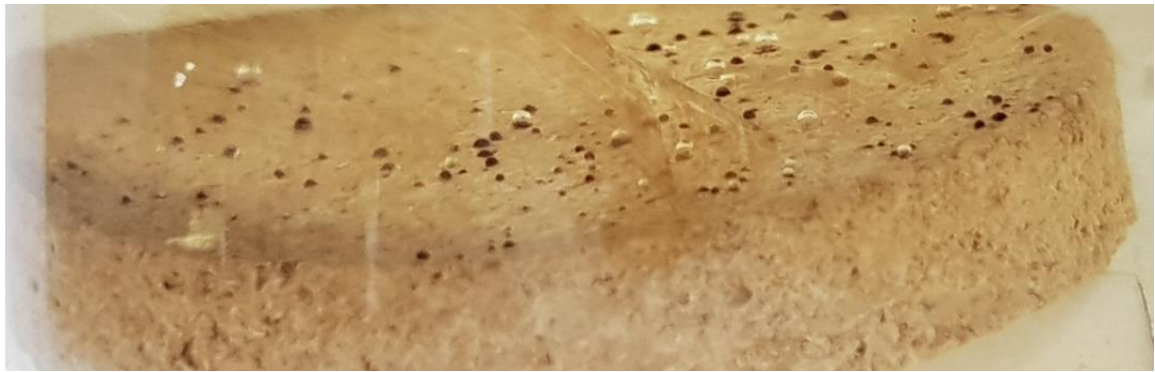


Figure A8 – Mackam® CB-35 initial screening.



Figure A9 – Ethoquad® 0/12 PG initial screening.

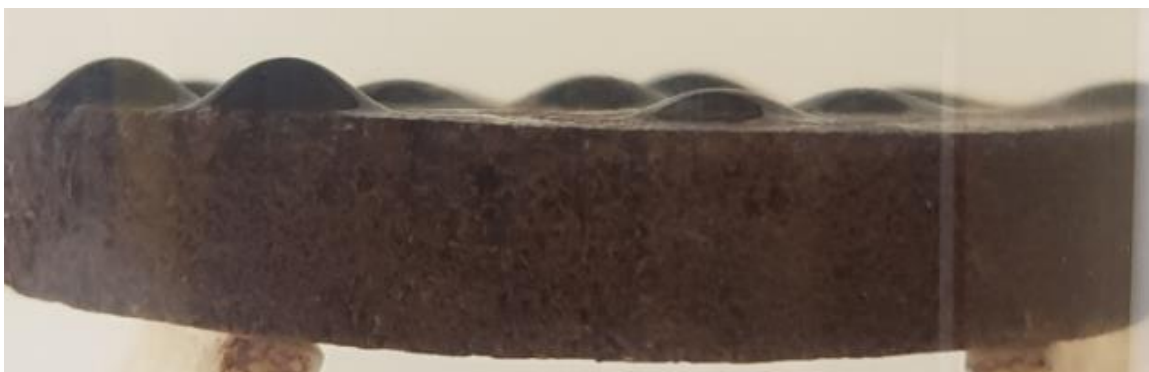


Figure A10 – Stepanquat® 3712-W initial screening.



Figure A11 – Benzalkonium Chloride initial screening.



Figure A12 – Phenol 2PO-60EO initial screening.



Figure A13 – Phenol 2PO-70EO initial screening.

REFERENCES

- Akbar, M. Vissapragada, B., and Alghamdi, A.H., et al. (2000). *A Snapshot of Carbonate Reservoir Evaluation*. Oilfield Review 12 (4), December, 20-41
- Anderson, W.G. (1986a). *Wettability Literature Survey Part 1: Rock/Oil/Brine Interactions and the Effects of Core Handling on Wettability*. Journal of Petroleum Technology, SPE, 38 (10), October, 1125-1144.
- Anderson, W.G. (1986b). *Wettability Literature Survey Part 2: Wettability Measurement*. Journal of Petroleum Technology, SPE, 38 (11), November, 1246-1262.
- Anderson, W.G. (1987a). *Wettability Literature Survey Part 4: Effects of Wettability on Capillary Pressure*. Journal of Petroleum Technology, SPE, 39 (10), October, 1283-1300.
- Anderson, W.G. (1987b). *Wettability Literature Survey Part 5: The Effects of Wettability on Relative Permeability*. Journal of Petroleum Technology, SPE, 39 (11), November, 1453-1468.
- Anderson, W.G. (1987c). *Wettability Literature Survey Part 6: The Effects of Wettability on Water Flooding*. Journal of Petroleum Technology, SPE, 39 (12), December, 1605-1622.
- Aoudia, M., Wade, W.H., and Weerasooriya, U. (1995). *Optimum Microemulsions Formulated with Propoxylated Tridecyl Alcohol Sodium Sulfates*. Journal of Dispersion Science and Technology 16 (2), April, 115-135.
- ATSM 664-89. (1989). *Standard Test Method for Acid Number Petroleum Products by Potentiometric Titration*, Annual Book of ATSM Standards, Section 5, American Society of Testing and Materials, Philadelphia.
- Austad, T. and Standnes, D.C. (2003). *Spontaneous Imbibition of Water into Oil-Wet Carbonates*. Journal of Petroleum Science and Engineering, 39 (3 & 4), 363-376.
- Barber, D.J., and Reeder, R.J. (1990). *Carbonates: Mineralogy and Chemistry*. Washington, D.C.: Mineralogical Society of America.
- Barnes, J.R., Goren, K., On, A., Dubey, S.T., Reznik, C., Buijse, M.A., and Shepherd, A.G. (2012). *Controlled Hydrophobe Branching to Match Surfactant to Crude Composition for Chemical EOR*. SPE-154084, presented at the Improved Oil Recovery Symposium, SPE, Tulsa, OK, 14-18 April
- Blake, T.D. and Kitchener, J.A. (1977). *Stability of Aqueous Films on Hydrophobic Methylated Silica*. Journal of Chemical Society, Faraday Transactions 1, 68, 1435-1442.
- Bourrel, M., and Schechter, R.S. (1988). *Microemulsions and Related Systems*. New York, NY: Marcel Dekker.

- Brownell, L.E. and Katz, D.L. (1947) *Flow of fluids through porous media*. Chemical Engineering Progress. 43 (10), 537-548.
- Buckley, J.S., Takamura, K., and Morrow, N.R. (1989). *Influence of Electrical Surface Charges on the Wetting Properties of Crude Oils*. SPE Reservoir Engineering, 4 (3), August, 332-333.
- Chatzis, I. and Morrow, N.R. (1983) *Correlation of Capillary Number Relationships for Sandstone*, SPE Journal 24 (5), October, 555-562.
- Chen, H.L., Lucas, L.R., Nogaret, L.A.D., Yang, H.D., Kenyon, D.E. (2000). *Laboratory Monitoring of Surfactant Imbibition Using Computerized Tomography*. SPE-59006, presented at the International Petroleum Conference and Exhibition, Society of Petroleum Engineers, Mexico, February 1-3.
- Chen, H.L., Lucas, R.L., Nogaret, L.A.D., Yang, H.D., and Kenyon, D.E. (2000). *Laboratory Monitoring of Surfactant Imbibition Using Computerized Tomography*. SPE-59006, presented at the International Petroleum Conference and Exhibition, SPE, Mexico, 1-3 February.
- Chen, P., and Mohanty, K.K. (2013). *Surfactant-mediated Spontaneous Imbibition in Carbonate Rocks at Harsh Reservoir Conditions*. SPE Journal, Society of Petroleum Engineers, 18 (1), January, 124-133.
- Chen, P., and Mohanty, K.K. (2014). *Wettability Alteration in High Temperature Carbonate Reservoirs*. SPE-169125, presented at the Improved Oil Recovery Symposium, SPE, Tulsa, OK., 12-16 April.
- Chu, Z., and Feng, Y. (2011). *Empirical Correlations between Krafft Temperature and Tail Length for Amidosulfobetaine Surfactants in the Presence of Inorganic Salt*. Langmuir, American Chemical Society, 28 (2), December, 1175-1181.
- Clementz, D.M. (1976). *Interaction of Petroleum Heavy Ends with Montmorillonite*. Clays and Clay Minerals, 24, December, 312-319
- Collins, S.H., and Melrose, J.C. (1983). *Adsorption of Asphaltenes and Water on Reservoir Rock Minerals*. SPE-11800, presented at the Oilfield and Geothermal Chemistry Symposium, SPE, Denver, CO., 1-3 June.
- Craig, F.F. (1971). *The Reservoir Engineering Aspects of Waterflooding*, Monograph Series, SPE, Richardson, TX.
- del Rio, J.M., Pombo, C., Mosquera, P.V., and Sarmiento, F. (1995). *Effect of Temperature and Alkyl Chain Length on the Micellar Properties of N-Alkyltrimethylammonium Bromides in a Low pH Medium*. Journal of Colloid and Interface Science, 172 (1), June, 137-141.
- Denekas, M.O, Mattax, C.C., and Davis, G.T. (1959). *Effect of Crude Oil Components on Rock Wettability*. Transactions of the AIME, 216 (1), December, 330-333.

- Donaldson, E.C., and Thomas, R.D. (1971). *Microscopic Observations of Oil Displacement in Water-Wet and Oil-Wet Systems*. SPE-3555, presented at Fall Meeting of the Petroleum Branch of AIME, SPE, New Orleans, LA., 3-6 October.
- Flaaten, A.K., Nguyen, Q.P., Pope, G.A., and Zhang, J. (2008). *A Systematic Laboratory Approach to Low-cost, High-performance Chemical Flooding*. SPE-113469, presented at the Improved Oil Recovery Symposium, SPE, Tulsa, OK., 20-23 April.
- Foster, W.R. (1973). *A Low-Tension Waterflooding Process*. Journal of Petroleum Technology, SPE, 25 (2), February, 205-210.
- Ghosh, P., Sharma, H., and Mohanty, K.K. (2017). *Chemical Flooding in Low Permeability Carbonate Rocks*. SPE-187274, presented at the Annual Technical Conference and Exhibition, SPE, San Antonio, TX, 9-11 October.
- Green, D.W. and Willhite, G.P. (1998). *Enhanced Oil Recovery*. Richardson, TX, USA: Society of Petroleum Engineers, 239-298.
- Gupta, R., and Mohanty K.K. (2008). *Wettability Alteration of Fractured Carbonate Reservoirs*. SPE-113407, presented at the Improved Oil Recovery Symposium, SPE, Tulsa, OK., 20-23 April.
- Gupta, R., Kshitji, M., and Mohanty, K.K. (2009). *Surfactant Screening for Wettability Alteration in Oil-wet Fractured Carbonates*. SPE-124822, presented at the Annual Technical Conference and Exhibition, Society of Petroleum Engineers, New Orleans, LA., 4-7 October.
- Gupta, S.P. and Trushenski, S.P. (1979). *Micellar Flooding – Compositional Effects on Oil Displacement*. SPE Journal 19 (2), April, 116-128.
- Hall, A.C., Collins, S.H., and Melrose, J.C. (1983). *Stability of the Aqueous Wetting Films in Athabasca Tar Sands*. SPE Journal, 23 (2), April, 249-259.
- Healy, R.N. and Reed, R.L. (1974). *Physiochemical Aspects of Microemulsion Flooding*. SPE Journal 14 (5), October, 491-501.
- Hirasaki, G.J. and Zhang, B., (2003). *Surface Chemistry of Oil Recovery from Fractured, Oil-Wet, Carbonate Formation*. SPE-80988, presented at the International Symposium on Oilfield Chemistry, SPE, Houston, TX, 5-8 February.
- Hirasaki, G.J., Miller, C.A., and Puerto, M. (2008) *Recent Advances in Surfactant EOR*. SPE-115386, presented at the Annual Technical Conference and Exhibition, SPE, Denver, CO, 21-22 September.
- Holm, L.W., and Robertson, S.D. (1981). *Improved Micellar/Polymer Flooding with High-pH Chemicals*. Journal of Petroleum Technology, Society of Petroleum Engineers, 33 (1), January, 161-171.

- Jadhunandan, P.P., and Morrow, N.R. (1995) *Effect of Wettability on Waterflood Recovery for Crude-Oil/Brine/Rock Systems*. SPE Reservoir Engineering, Society of Petroleum Engineers, 10 (1), February, 40-46.
- Jennings, H.Y. Jr. (1957). *Surface Properties of Natural and Synthetic Porous Media*. Producers Monthly, 21 (5), March, 20-24.
- Kamath, J., Meyer, R.F., and Nakagawa, F.M (2001). *Understanding Waterflood Residual Oil Saturation of Four Carbonate Rock Types*. SPE-71505, presented at the Annual Technical Conference and Exhibition, SPE, New Orleans, LA., 30 September – 3 October.
- Kumar, K., Dao, E.K., and Mohanty, K.K. (2008). *Atomic Force Microscopy Study of Wettability Alteration by Surfactants*. SPE Journal 13 (2), June, 137-145.
- Lake, L.W., Johns, R.T., Rossen, W.R., and Pope, G.A. (2014). *Fundamentals of Enhanced Oil Recovery*. Second ed., Society of Petroleum Engineers.
- Lefebvre du Prey, E.J. (1973). *Factors Affecting Liqui-Liquid Relative Permeabilities of a Consolidated Porous Medium*. SPE Journal, 13 (1), February, 39-47.
- Levitt, D.B, Jackson, A.C., Heinson, C., Britton, L.N., Malik, T., Dwarakanath, V., and Pope, G.A. (2006). *Identification and Evaluation of High Performance EOR Surfactants*. SPE-100089, presented at the Symposium on Improved Oil Recovery, SPE/DOE, Tulsa, OK., 22-26 April.
- Ma, S., Morrow, N.R., and Zhang, X. (1995). *Generalized Scaling of Spontaneous Imbibition Data for Strongly Water-Wet Systems*. PETSOC-95-138, presented at the Technical Meeting / Petroleum Conference of The South Saskatchewan Section, Petroleum Society of Canada, October 16-18, Regina.
- Manrique, E.J., Muci, V.E., and Gurfinkel, M. E. (2006). *EOR Field Experiences in Carbonate Reservoirs in the United States*. SPE-100063, presented at the Improved Oil Recovery Symposium, SPE, Tulsa, OK., 22-26 April.
- Mattax, C.C. and Kyte, J.R. (1961). *Ever See a Waterflood?* Oil & Gas Journal, 59 (42), October, 115-128.
- McCaffery, F.G., Bennion, D.W. (1974). *The Effect of Wettability on Two-Phase Relative Permeabilities*. Journal of Canadian Petroleum Technology, Petroleum Society of Canada, 13 (4), October, 42-53.
- Mohanty, K.K., Davis, H.T., Scriven, L.E. (1987). *Physics of Oil Entrapment in Water-Wet Rock*. SPE Reservoir Engineering, Society of Petroleum Engineers, 2 (1), February, 113-128.
- Moore, T.F., and Slobod, R.L. (1955). *Displacement of Oil by Water – Effect of Wettability, Rate, and Viscosity on Recovery*. SPE-502-G, presented at Fall Meeting of the Petroleum Branch of AIME, SPE, New Orleans, LA., 2-5 October.

- Morrow, N.R. (1979). *Interplay of Capillary, Viscous, and Buoyance Forces in the Mobilization of Residual Oil*. Journal of Canadian Petroleum Technology, Petroleum Society of Canada, 18 (3), July - September, 35-46.
- Morrow, N.R. (1990). *Wettability and its Effect on Oil Recovery*. Journal of Petroleum Technology, SPE, 42 (12), December, 1476-1484.
- Morrow, N.R. and Mason, G. (2001). *Recovery of Oil by Spontaneous Imbibition*. Current Opinion in Colloid & Interface Science, 6 (4), August, 321-337.
- Myers, D. 2006. *Surfactant Science and Technology*. 3rd ed. Hoboken, N.J: J. Wiley.
- Nakama, Y., Harusawa, F., and Murotani, I. (1990). *Cloud Point Phenomena in Mixtures of Anionic and Cationic Surfactants in Aqueous Solution*. Journal of the Americal Oil Chemists' Society, 67, November, 717-721.
- Nelson, R.C. and Pope, G.A. (1978). *Phase Relationships in Chemical Flooding*. SPE Journal, 18 (5), 325-338.
- Nelson, R.C. (1981). *Further Studies on Phase Relations in Chemical Flooding*. Surface Phenomena in Enhanced Oil Recovery by Shah, D.O., Plenum Press, NY, 73-104.
- Nieto-Alvarez, D.A., Zamudio-Rivera, L.S., Luno-Rojero, E.E., Rodriguez-Otamendi, D.I., Marin-Leon, A., Hernandez-Altamirano, R., Mena-Cervantes, V.Y., and Chavez-Miyauchi, T.E. (2012). *Adsorption of Zwitterionic Surfactant on Limestone Measured with High-Performance Liquid Chromatography: Micelle-Vesicle Influence*. Langmuir, American Chemical Society, 30 (41), 12243-12249.
- Owens, W.W. and Archer, D.L. (1971). *The Effect of Rock Wettability on Oil-Water Relative Permeability Relationship*. Journal of Petroleum Technology, SPE, 23 (7), July, 873-878.
- Raza, S.H, Trebeir, L.E., and Archer, D.L. (1968). *Wettability of Reservoir Rocks and Its Evaluation*. Producers Monthly, 32 (4), April, 2-7.
- Salathiel, R.A. (1973). *Oil Recovery by Surface Film Drainage in Mixed-Wettability Rocks*. Journal of Petroleum Technology, SPE, 25 (10), October, 1216-1224.
- Schechter, D.S., Zhou, D., and Orr, F.M., Jr. (1994). *Low IFT Drainage and Imbibition*. Journal of Petroleum Science and Engineering (11), 283-300.
- Seethepalli, A., Adibhatla, B., and Mohanty, K. K., (2004). *Physicochemical Interactions During Surfactant Flooding of Fractured Carbonate Reservoirs*. SPE Journal 9 (4), December, 411-418.
- Sharma, G., and Mohanty, K. K. (2013). *Wettability Alteration in High-Temperature and High-Salinity Carbonate Reservoirs*. SPE Journal 18 (4), April, 646-655.
- Solairaj, S., Britton, C., Lu, J., Kim, D.H, Weerasooriya, U., and Pope, G.A. (2012). *New Correlation to Predict Optimum Surfactant Structure for EOR*. SPE-154262,

- presented at the Improved Oil Recovery Symposium, SPE, Tulsa, OK, 14-18 April.
- Spinler, E.A., and Baldwin, B.A. (2000). *Surfactant Induced Wettability Alteration in Porous Media*. Surfactants: Fundamentals and Applications in the Petroleum Industry, Schramm, L.L. Cambridge University Press: Cambridge, UK. 159-202.
- Standnes, D.C., and Austad, T. (2000). *Wettability Alteration in Chalk: 2. Mechanism for Wettability Alteration from Oil-Wet to Water-Wet Using Surfactants*. Journal of Petroleum Science and Engineering 28 (3), 123-143.
- Standnes, D.C., and Austad, T. (2003). *Wettability Alteration in Carbonates Interaction Between Cationic Surfactants and Carboxylates as a Key Factor in Wettability Alteration from Oil-Wet to Water-Wet Conditions*. Colloids and Surfaces A: Physiochemical and Engineering Aspects, 216, 243-259.
- Stegemeier, G. (1977). *Mechanisms of Entrapment and Mobilization of Oil in Porous Media*. Improved Oil Recovery by Surfactant and Polymer Flooding, 55-91
- Taber, J.J. (1969). *Dynamic and Static Forces Required to Remove a Discontinuous Oil Phase from Porous Media Containing Both Oil and Water*. SPE Journal 9 (1), March, 3-12.
- Treiber, L.E., Archer, D.L., and Owens, W.W. (1972). *A Laboratory Evaluation of The Wettability of Fifty Oil-Producing Reservoirs*. SPE Journal 12 (6), December, 531-540.
- Van Golf-Racht, T.D. (1982). *Fundamentals of Fractured Reservoir Engineering*. Elsevier Science Publishing Co., New York City, Ny.
- Wardlaw, N.C. (1982) *The Effects of Geometry, Wettability, Viscosity, and Interfacial Tension on Trapping in Single Pore-Throat Pairs*. Journal of Canadian Petroleum Technology, Petroleum Society of Canada, 21 (3), May - June, 21-27.
- Wardlaw, N.C. (1996). *Factors Affecting Oil Recovery from Carbonate Reservoirs and Prediction of Recovery. Carbonate Reservoir Characterization: A Geologic Engineering Analysis, Part II*: Elsevier Science BV. 867-903.
- Warren, J.E., and Calhoun, J.C. Jr. (1955) *A Study of Waterflood Efficiency in Oil-Wet Systems*. Transactions of the AIME, SPE, 204 (1), December, 1955.
- Washburn, E.W. (1921). *The Dynamics of Capillary Flow*. Physical Review, American Physical Society, 17 (3), March, 273-283.
- Weiss, W.W., Xie, X., Weiss, J., Subramaniam, V., Taylor, A., and Edens, F. (2004). *Artificial Intelligence Used to Evaluate 23 Single-well Surfactant Soak Treatments*. SPE-89457, presented at the Symposium on Improved Oil Recovery, SPE/DOE, Tulsa, OK, 17-21 April.

- Wilson, D., Poindexter, L., and Nguyen, T. (2019). *Role of Surfactant Structures on Surfactant-Rock Adsorption in Various Rock Types*. SPE-193595, presented at the International Conference on Oilfield Chemistry, SPE, Galveston, TX., 8-9 April.
- Xie, X., Weiss, W.W., Tong, Z.J., and Morrow, N.R. (2005). *Improved Oil Recovery from Carbonate Reservoirs by Chemical Stimulation*. SPE Journal, Society of Petroleum Engineers, 10 (3), September, 276-285.
- Zhang, D.L., Liu, S., Puerto, M. Miller, C.A., and Hirasaki, G. J. (2006). *Wettability Alteration and Spontaneous Imbibition in Oil-Wet Carbonate Formations*, Journal of Petroleum Science and Engineering. 52 (1), June, 213-226.
- Zhang, Y., Yue, X., Dong, J., and Liu, Y. (2000). *New and Effective Foam Flooding to Recover Oil in Heterogenous Reservoir*. SPE-59367, presented at the Improved Oil Recovery Symposium, SPE/DOE, Tulsa, OK, 3-5 April.
- Zhang, B. and Austad, T. (2015). *The Relative Effects of Acid Number and Temperature on Chalk Wettability*. SPE-92999, presented at the International Symposium on Oilfield Chemistry, SPE, Houston, TX, 2-4 February.
- Zhou, X., Xie, X., and Marrow, N.R. (1995). *The Effect of Crude-Oil Aging Time and Temperature on the Rate of Water Imbibition and Long-Term Recovery by Imbibition*. SPE Formation Evaluation, 10 (4), December, 259-265.